Parasitology Research (2019) 118:3279–3305
https://doi.org/10.1007/s00436-019-06476-7

FISH PARASITOLOGY - ORIGINAL PAPER

Myxozoan biodiversity in mullets (Teleostei, Mugilidae) unravels hyperdiversification of *Myxobolus* (Cnidaria, Myxosporea)

Sónia Rocha[1,2] · Graça Casal[3] · Ângela Alves[1] · Carlos Antunes[2,4] · Pedro Rodrigues[1,5,6] · Carlos Azevedo[1,2]

Received: 4 December 2018 / Accepted: 24 September 2019 / Published online: 1 November 2019

Abstract

Mullets are ecologic and commercially important fish species. Their ubiquitous nature allows them to play critical roles in freshwater and marine ecosystems but makes them more vulnerable to diseases and parasitic infection. In this study, a myxozoan survey was performed on three species of mullet captured from a northern Portuguese river. The results disclose a high biodiversity, specifically due to the hyperdiversification of *Myxobolus*. Thirteen new species of this genus are described based on microscopic and molecular procedures: 7 from the thinlip grey mullet *Chelon ramada*, 2 from the thicklip grey mullet *Chelon labrosus*, and 4 from the flathead grey mullet *Mugil cephalus*. *Myxobolus exiguus* and *Ellipsomyxa mugilis* are further registered from their type host *C. ramada*, as well as six more myxospore morphotypes that possibly represent distinct *Myxobolus* species. Overall, the results obtained clearly show that the number of host-, site- and tissue-specific *Myxobolus* spp. is much higher than what would be expected in accordance to available literature. This higher biodiversity is therefore discussed as either being the result of the usage of poor discriminative criteria in previous studies, or as being a direct consequence of the biological and ecological traits of the parasite and of its vertebrate and invertebrate host communities. Bayesian inference, maximum likelihood and maximum parsimony analyses position the new species within a clade comprising all other *Myxobolus* spp. that infect mugiliform hosts, thus suggesting that this parasitic group has a monophyletic origin. Clustering of species in relation to the host genus is also revealed and strengthens the contention that the evolutionary history of mugiliform-infecting *Myxobolus* reflects that of its vertebrate hosts. In this view, the hyperdiversification of *Myxobolus* in mullet hosts is hypothesized to correlate with the processes of speciation that led to the ecological plasticity of mullets.

Keywords Mugiliformes · *Myxobolus*-richness · *Ellipsomyxa mugilis* · Phylogeny · SSU rDNA gene · Portugal

Introduction

The family Mugilidae, whose members are commonly known as mullets, is one of the most ubiquitous among euryhaline teleosts, containing about 70 species that are distributed in marine, brackish and freshwater habitats of tropical, subtropical and temperate regions worldwide (Hotos and Vlahos 1998; Cardona 2001; Durand et al. 2012; Nelson et al.

Section Editor: Christopher Whipps

Electronic supplementary material The online version of this article (https://doi.org/10.1007/s00436-019-06476-7) contains supplementary material, which is available to authorized users.

✉ Sónia Rocha
sonia.oliveira.rocha@gmail.com

[1] Institute of Biomedical Sciences Abel Salazar, University of Porto, Rua Jorge Viterbo Ferreira no. 228, 4050-313 Porto, Portugal

[2] Interdisciplinary Centre of Marine and Environmental Research (CIIMAR), University of Porto, Terminal de Cruzeiros de Leixões, Av. General Norton de Matos s/n, 4450-208 Matosinhos, Portugal

[3] University Institute of Health Sciences & Institute of Research and Advanced Training in Health Sciences and Technologies, CESPU, Rua Central da Gandra no. 1317, 4585-116 Gandra, Portugal

[4] Aquamuseu do Rio Minho, Parque do Castelinho, 4920-290, Vila Nova de Cerveira, Portugal

[5] Institute for Molecular and Cell Biology (IBMC), University of Porto, Rua Alfredo Allen no. 208, 4200-135 Porto, Portugal

[6] Instituto de Investigação e Inovação em Saúde (i3S), University of Porto, Rua Alfredo Allen no. 208, 4200-135 Porto, Portugal

2016). The ecological plasticity of mullets is not restricted to habitat, as their omnivorous nature and benthic feeding strategy allows them to feed on a great variety of materials, including epiphytic algae, insects, annelids, crustaceans, mollusks and even detritus (Cardona 2001; Laffaille et al. 2002; Almeida 2003). Consequently, these fishes carry out decisive roles in their ecosystems, namely in the energy and matter flow from the lower to the upper levels, but are also more vulnerable to diseases and parasitic infection (Paperna and Overstreet 1981; Laffaille et al. 2002; Almeida 2003; Zetina-Rejón et al. 2003; Rocha et al. 2019a). In turn, the commercial importance of mullets varies with geographic location; nonetheless, its global production for human consumption is an increasing trend (Oren 1981; Crosetti and Cataudella 1995; Saleh 2006). In the Mediterranean, these fishes have been considered an important food source since the Roman period (Crosetti 2016). The production of mullets depends on the acquisition of fry or fingerlings from natural stocks, which contributes to an increasing interest in studying the parasitic community infecting wild populations.

Myxozoans are parasitic cnidarians that diversified extensively in aquatic ecosystems, mainly using fish as their temporary vertebrate hosts (Holzer et al. 2018). Considering that many species of this group represent ecologic and economic threats to wild and reared fish populations, studying myxozoan biodiversity in mullets is crucial for the sustainability of natural stocks and increment of aquaculture production. During the past century, several studies have aimed to provide information regarding the myxozoan community parasitizing mullets, with ca. 80 species of the class Myxosporea Bütschli, 1881 thus far described from these hosts in different geographic locations. Of these, about 38 are species of the family Myxobolidae Thélohan, 1892, predominantly of the genus *Myxobolus* Bütschli, 1882, while the remaining are distributed among genera of the families: Alatasporidae Schulman et al., 1979; Ceratomyxidae Doflein, 1899; Chloromyxidae Thélohan, 1892; Kudoidae Meglitsch, 1960; Myxidiidae Thélohan, 1892; Myxobilatidae Shulman, 1953 [currently includes the genus *Ortholinea*, as a result of the dismantling of the family Ortholineidae (Karlsbakk et al. 2017)]; Sinuolineidae Shulman, 1959; Sphaeromyxidae Lom and Noble, 1984; and Sphaerosporidae Davis, 1917 (see Yurakhno and Ovcharenko 2014; Barreiro et al. 2017; Yang et al. 2017; Rocha et al. 2019a).

In the Iberian Peninsula, 11 *Myxobolus* spp. have been reported to occur in mugilid hosts, mostly from the Mediterranean waters off the Spanish Eastern coast. *Myxobolus adeli* (Isjumova, 1964) Yurakhno and Ovcharenko, 2014 was originally described from the Iberian Peninsula, parasitizing the digestive tract, swim bladder, gills and muscles of golden grey mullet *Chelon auratus* (Risso, 1810) in the Ebro Delta and Santa Pola Bay, Spain (see Yurakhno and Ovcharenko 2014). *Myxobolus exiguus* Thélohan, 1895 was morphologically re-described from the visceral peritoneum of thinlip grey mullet *Chelon ramada* (Risso, 1827) in a northern Portuguese River (Minho) (Rocha et al. 2019a), having been identified based on molecular information of the SSU rDNA gene. In turn, *Myxobolus episquamalis* Egusa et al., 1990, *Myxobolus ichkeulensis* Bahri and Marques, 1996, *Myxobolus nile* Negm-Eldin et al., 1999 and *Myxobolus rohdei* Lom and Dyková, 1994, were reported to be present in this geographic region solely on the basis of myxospore morphological traits (see Yurakhno and Ovcharenko 2014). The remaining five *Myxobolus* spp. are unnamed, having been recently molecularly described from *Mugil cephalus* Linnaeus, 1758 in the Spanish Mediterranean coast (Sharon et al. 2019).

In addition to these *Myxobolus* species, *Ellipsomyxa mugilis* Sitjà-Bobadilla and Álvarez-Pellitero, 1993, *Kudoa trifolia* Holzer et al., 2006, *Kudoa unicapsula* Yurakhno et al., 2007, *Sphaerospora mugilis* Sitjà-Bobadilla and Álvarez-Pellitero, 1995, and a species of the genus *Alataspora* Schulman et al., 1979 were also originally described from mullets inhabiting Spanish Mediterranean coastal waters (see Sitjà-Bobadilla and Álvarez-Pellitero 1993, 1995; Holzer et al. 2006; Yurakhno et al. 2007; Yurakhno and Ovcharenko 2014). Yurakhno and Ovcharenko (2014) further reported the occurrence of *Enteromyxum leei* Diamant et al., 1994, *Sphaeromyxa sabrazesi* Laveran and Mesnil, 1900, *Kudoa dicentrarchi* Sitjà-Bobadilla and Álvarez-Pellitero, 1992, and *Zschokkella admiranda* Yurakhno, 1993 in mullets from this geographic location, having identified these species based on the morphological traits of their myxospores. Thus, with the exception of the occurrence of *M. exiguus* in *C. ramada* from the River Minho (Rocha et al. 2019a), and of actinosporean stages of *E. mugilis* infecting the polychaete *Hediste diversicolor* Müller, 1776 in the Aveiro estuary (Rangel et al. 2009), to our best knowledge nothing more is known about the myxozoan community infecting mullets in the Atlantic coastal waters of Portugal.

The River Minho marks the boundaries between northern Portugal and Spain. It originates in "Serra da Meira", in the province of Lugo (Spain) and runs more than 300 km to drain into the Atlantic Ocean at the Portuguese northwest coast near the city of Caminha. This freshwater ecosystem has great ecologic and economic importance at a regional level; however, its biodiversity is threatened by the synergetic effects of habitat loss, introduction of non-native species, climate change, impoundments and river regulations, fishing activities and pollution. Mullets are no exception, being subjected to these natural and anthropogenic pressures. Also, despite their relatively regionally low commercial value, mullets in the River Minho are commercially exploited, providing a source of income for local fishermen (Sousa et al. 2008; Mota et al. 2016). Overall, the River Minho is home to four species of mullets: the golden grey mullet *C. auratus*, the thinlip grey mullet

C. ramada, the thicklip grey mullet *Chelon labrosus* (Risso, 1827) and the flathead grey mullet *M. cephalus*. Co-habitation is made possible by the capability of mugilid species to utilize different energy sources (Crosetti and Cataudella 1995). In coastal and estuarine systems, the salinity gradients also allow a zonal distribution of mugilids (Cardona 2006) and a day and night turnover of different species has been reported to further support co-habitation (Torricelli et al. 1981). Consequently, all four species may be present throughout the year in the River Minho with highest incidence during the summer period. However, it is *C. ramada* that gets caught more often in upstream locations, due to its high adaptability to low salinities and water pollution (Cardona 2006). In this study, a myxozoan survey conducted on mullets captured from the River Minho disclosed a high biodiversity of *Myxobolus*, with a total of thirteen new species described using microscopic and molecular tools. Phylogenetic analyses using Bayesian inference, maximum likelihood and maximum parsimony methodologies revealed the monophyletic origin of mugiliform-infecting myxobolids and corroborated the evolutionary hyperdiversification of *Myxobolus* within mullet hosts.

Materials and methods

Fish sampling and myxozoan survey

Between 2013 and 2018, trimestral samplings of fishes were performed from fyke-nets located in the River Minho (41° 56′ N, 08° 45′ W), near "Vila Nova de Cerveira", Portugal. Fish samples included species of the orders Anguilliformes, Atheriniformes, Cypriniformes, Perciformes, Pleuronectiformes and Mugiliformes. Mugilids were represented by specimens of the thinlip grey mullet *Chelon ramada* (Risso, 1827) [$n = 22$; total length 20.3 ± 11.4 (10.5–41.2) cm; weight 137 ± 201 (9–601) gr], the thicklip grey mullet *Chelon labrosus* (Risso, 1827) [$n = 3$; total length 44.0 ± 2.1 (42.5–45.5) cm; weight 884 ± 13 (875–893) gr], and the flathead grey mullet *Mugil cephalus* Linnaeus, 1758 [$n = 10$; total length 40.6 ± 6.8 (33.5–53.0) cm; weight 759 ± 376 (440–1582) gr]. Fish were transported live to the laboratory and anaesthetized with ethylene glycol monophenyl ether (Merck, Germany) at 1 ml/L. Upon dissection, fish specimens were surveyed for the presence of myxozoan parasites in several organs and tissues, specifically: brain; eye and ocular cavity; tegument and scales; gills and opercular cavity; skeletal muscle; heart; liver; gall bladder; spleen; gonads; swim bladder; kidney; urinary bladder and digestive tube.

Microscopic analysis and morphological examination

All collected cysts and parasitized tissues were photographed using an Olympus BX50 light microscope (Olympus, Japan) in order to determine the morphology and morphometry of the myxospores from fresh material, following the guidelines provided by Lom and Arthur (1989). Co-infections were primarily determined microscopically through the morphometric traits of the myxospores. Tissue samples did not proceed for molecular analyses whenever evidence of infection by more than a single morphological type of myxospore was found, except if these belonged to morphologically distinguishable myxozoan genera (e.g. *Myxobolus* and *Ellipsomyxa*). All measurements herein provided include the mean value ± standard deviation (S.D.), range of variation and number of myxospores measured (range, *n*).

DNA extraction, amplification and sequencing

Samples of cysts or fragments of parasitized tissue were fixed and preserved in 80% ethanol at 4 °C. Genomic DNA was extracted from samples without microscopic evidence of co-infection by members of the same genus. Extractions were performed using a GenElute™ Mammalian Genomic DNA Miniprep Kit (Sigma-Aldrich, St Louis, USA), according to the manufacturer's instructions.

The SSU rDNA gene was amplified and sequenced using both universal and myxosporean-specific primers (Table 1), so that all partial sequences overlapped in several regions. PCRs were performed in 50-μl reactions using 10 pmol of each primer, 10 nmol of dNTPs, 2 mM $MgCl_2$, 5 μl 10× *Taq* polymerase buffer, 2.5 units *Taq* DNA polymerase (NZYTech, Lisbon, Portugal), and approximately 50–100 ng of genomic DNA. PCRs were run on a Hybaid PxE Thermocycler (Thermo Fisher Scientific, Waltham, Massachusetts, EUA), with initial denaturation at 95 °C for 3 min, followed by 35 cycles of 94 °C for 45 s, 53 °C for 45 s and 72 °C for 90 s. The final elongation step was performed at 72 °C for 7 min. Five-microliter aliquots of the PCR products was electrophoresed through a 1% agarose 1× tris-acetate-EDTA buffer (TAE) gel stained with ethidium bromide. PCR products were purified using Puramag™ magnetic beads coated with carboxylic acid groups (MCLAB, San Francisco, California, USA).

The PCR products from different regions of the SSU rDNA gene were sequenced directly. Sequencing reactions were performed using a BigDye Terminator v3.1 Cycle Sequencing Kit from AppliedBiosystems (Thermo Fisher Scientific, Waltham, Massachusetts, EUA), and were run on an ABI3700 DNA analyser from AppliedBiosystems (Thermo Fisher Scientific, Waltham, Massachusetts, EUA).

Sequence assembly, distance estimation, and phylogenetic analysis

The partial sequences obtained for each case isolate were aligned in MEGA 7 (Kumar et al. 2016) for the construction of the respective assembled SSU rDNA sequences. Tissue

Table 1 Polymerase chain reaction primers used for the amplification and sequencing of the SSU rDNA gene

Name	Sequence (5′-3′)	Paired with	Source
18E	CTG GTT GAT CCT GCC AGT	MyxospecR, ACT2r, ACT3r, MYX4R	Hillis and Dixon (1991)
MyxospecF	TTC TGC CCT ATC AAC TTG TTG	MYX4R, 18R	Fiala (2006)
ACT2f	CCT GGT CCG AAC ATC CGA AGG ATA C	18R	This study
ACT3f	CAT GGA ACG AAC AAT	18R	Hallett and Diamant (2001)
ACT5f	TGT GCC TTG AAT AAA T	18R	Rocha et al. (2019b)
MYX4F	GTT CGT GGA GTG ATC TGT CAG	18R	Hallett and Diamant (2001); Rocha et al. (2015)
MyxospecR	CAA CAA GTT GAT AGG GCA GAA	18E	Fiala (2006)
ACT2r	GTA TCC TTC GGA TGT TCG GAC CAG G	18E	This study
ACT3r	ATT GTT CGT TCC ATG	18E	Rocha et al. (2014)
MYX4R	CTG ACA GAT CAC TCC ACG AAC	18E, MyxospecF	Hallett and Diamant (2001)
18R	CTA CGG AAA CCT TGT TAC G	MyxospecF, ACT2f, ACT3f, MYX4F	Whipps et al. (2003)

samples were regarded as unreliable, or as possible co-infections, whenever the obtained partial sequences incorporated overlapping peaks, low-quality peaks, or suspect base-calling errors in regions other than at the extremities. A preliminary alignment was performed for the numerous novel assembled SSU rDNA sequences, using software MAFFT version 7 available online. Sequences determined to be identical between different case isolates were used to calculate prevalence of infection.

For distance estimation, datasets were generated according to the highest similarity scores obtained using BLAST search. One dataset included the SSU rDNA sequences of the 13 new *Myxobolus* spp. described here, as well as all others available for *Myxobolus* spp. that have *bona fide* mugiliform fish hosts (see Rocha et al. 2019a), and those of phylogenetically related actinosporean stages i.e. sphaeractinomyxon, endocapsa, and the Triactinomyxon of Székely et al., 2007 (DQ473515). Another dataset comprised all available SSU rDNA sequences for species of the genus *Ellipsomyxa*. Sequences were aligned using MAFFT version 7, and distance estimation was calculated in MEGA 7, with the *p*-distance model and all ambiguous positions removed for each sequence pair.

For the phylogenetic analysis of the new *Myxobolus* spp., only the SSU rDNA sequences of myxosporean stages were kept. The final dataset comprised a total of 24 SSU rDNA sequences, including *Myxobolus cerebralis* (U96492) and *Myxobolus wulii* (KP642131) as outgroup. Sequences were aligned using software MAFFT version 7 available online, and manually edited in MEGA 7. Phylogenetic trees were calculated using Bayesian inference (BI), maximum-likelihood (ML) and maximum parsimony (MP) methodologies. ML and MP analyses were conducted in MEGA 7, with bootstrap values calculated from 1000 replicates. For ML, the general time reversible substitution model with estimates of invariant sites and gamma distributed among site rate variation (GTR + I +G) was chosen as the best suited model, based on the lowest score of Bayesian Information Criterion (BIC) and corrected Akaike Information Criterion (AIC) with the MEGA package. For MP, the Subtree-Pruning-Regrafting algorithm was used, with a search level of 1 and random initial tree addition of 10 replicates. BI analyses were performed using MrBayes v3.2.6 (Ronquist and Huelsenbeck 2003); posterior probability distributions were generated using the Markov Chain Monte Carlo method, with four chains running simultaneously, for 500,000 generations, and every 100th tree sampled.

Results

Collected and analysed fish did not display obvious external signs of infection or disease. Macro- and microscopic analyses for the detection of myxozoan parasites revealed the presence of myxospores in multiple organs and tissues, appearing either disseminated or contained within plasmodia or cysts. Myxospores were all morphologically identified as belonging to the genus *Myxobolus* (Myxosporea, Myxobolidae), with the exception of a species of the genus *Ellipsomyxa* (Myxosporea, Ceratomyxidae) parasitizing the gall bladder of *C. ramada*. Another myxosporean species belonging to an undetermined genus was also found in the intestine of several specimens of *C. ramada*. The data acquired for this latter species remains, at this point, insufficient for its proper characterization.

All 22 specimens of *C. ramada* displayed infection by *Myxobolus* spp. in at least one of the organs and tissues analysed, with co-infections by members of this genus taking place in the gills, spleen, gall bladder, kidney and digestive tube (see Table 2). Myxosporean infection was never detected in the tegument, scales, brain, eyes, gonads and swim bladder of this fish host. A total of six specimens displayed further cysts developing attached to the visceral peritoneum, which

Table 2 *Myxobolus* infection in the different organs of the 22 specimens of *C. ramada* examined, as determined by light microscopic observations. PI: overall prevalence of infection of *Myxobolus* per organ examined; Ma: *M. adiposus* n. sp.; Mr: *M. ramadus* n. sp.; Mp: *M. pharyngobranchialis* n. sp.; Mm: *M. muscularis* n. sp.; Mh: *M. hepatobiliaris* n. sp.; Me: *M. exiguus*; Mren: *M. renalis* n. sp.; Mc: *M. cerveirensis* n. sp.; Mh?/Mren?/Mc?: myxospores consistent with the morphology of the species described here from the organ in question, but which identity could not be molecularly confirmed; M1–M6: unidentified *Myxobolus* spp. 1 to 6

Specimen#	Ocular cavity	Gills	Opercular cavity	Skeletal muscle	Heart	Liver	Gall bladder	Spleen	Kidney	Urinary bladder	Digestive tube
1	Ma	–	–	–	–	–	–	–	Mren?	–	–
2	–	–	–	–	–	Mh	–	–	–	–	M5, M6
3	–	–	–	–	–	–	–	–	M4	–	–
4	–	Mr	–	–	–	–	–	–	–	–	–
5	–	–	–	–	–	–	–	–	Mren?, M4	–	–
6	Ma	–	–	–	–	–	–	–	–	Ma	–
7	–	–	–	–	–	–	–	–	–	–	M5, M6
8	–	–	–	–	–	–	–	–	Mren?, M4	–	–
9	–	–	–	–	–	–	–	–	–	–	Mc
10	–	–	Mp	–	–	–	–	–	–	–	–
11	–	Mr, M1	–	–	–	–	–	–	Mren?, M4	–	–
12	–	–	–	–	–	–	Me[a]	–	Mren	–	M5, Me
13	Ma	–	–	–	–	–	–	M2, M3	–	–	M5, M6
14	–	Mr	–	Mm	Mm	–	Me[a]	–	Mren	–	Mc?, M5
15	–	–	–	–	Mm	–	Mh	–	–	–	Mc?, M5, M6
16	–	Mr, M1	–	–	–	–	–	–	Mren	–	Mc?, M6
17	–	–	–	–	–	–	Me	–	–	–	Mc?, M5, M6[b]
18	–	–	Mp	–	–	–	Me[a]	M2, M3	Mren?, M4	–	–
19	–	–	–	–	–	–	Me[a]	–	–	–	Mc?[c]
20	–	–	Mp	Mm	–	–	Mh?, Me[a]	–	–	–	Mc?, M5, Me[b]
21	Ma	–	Mp	–	–	–	–	–	Mren?, M4	Ma	–
22	Ma	–	Mp	–	–	–	–	–	–	–	–
PI	22.7%	18.2%	22.7%	9.1%	9.1%	4.5%	27.3%	9.1%	45.4%	9.1%	50.0%

[a] Co-infection with *Ellipsomyxa mugilis*

[b] Co-infection with a myxosporean species of an undetermined genus

[c] Co-infection was molecularly determined

morphological and molecular analysis identified as *M. exiguus* [data published in Rocha et al. 2019a].

At least three different morphotypes of *Myxobolus* were observed either forming plasmodia or appearing disseminated in the digestive tube, mostly in the intestine. Co-infection by two or three of these morphotypes was microscopically determined in nine out of the 11 specimens displaying infection in the digestive tube. Contamination with myxospores of *M. exiguus* due to rupture of microscopic cysts in the visceral peritoneum was further registered in specimens #12 and #20 (see Table 2). In total, only the parasitized intestinal samples belonging to specimens #9 and #19 were without microscopic signs of co-infection and, therefore, proceeded for molecular analyses (see Table 2). The partial SSU rDNA sequences obtained from the intestinal samples of specimen #19, however, incorporated many overlapping peaks and suspect base-calling errors, suggesting them as being unreliable. Thus, only the data obtained from specimen #9 was used to describe here a new *Myxobolus* species from the intestine of *C. ramada*.

Two morphologically distinguishable myxospores of *Myxobolus* were observed developing in five out of the 10 specimens displaying kidney infection (see Table 2). Despite being without microscopic evidence of co-infection, samples belonging to specimens #1 and #3 could not be used for molecular procedures due to the very low intensity of the infection, associated with obvious aspects of lysis of the myxospores. Molecular analysis of kidney samples belonging to specimens #12, #14 and #16 originated 100% identical SSU rDNA partial sequences, allowing the description of a new *Myxobolus* species from this organ.

In the same manner, two species of *Myxobolus* were observed forming cysts in the gills of *C. ramada* (see Table 2).

One species formed whitish and filamentous cysts developing in the gill lamellae of all four specimens with infection in this organ, while a second species formed brownish and filamentous cysts in the afferent artery of the gill filaments of only specimens #11 and #16. The cysts developing in the gill lamellae reached macroscopic dimensions (2–3 mm in length) and could be easily excised and isolated, allowing the species to be described here. In turn, the species developing in the afferent artery of the gill filaments could not be described as a result of the microscopic size of its cysts. Attempts to isolate them were not successful, since the SSU rDNA partial sequences obtained from respective DNA extractions incorporated overlapping peaks and suspect base-calling errors.

In the gall bladder, two morphotypes of *Myxobolus* were also observed, one having myxospores overall bigger than the other: the bigger myxospores appeared floating free in the bile, while the smaller myxospores formed plasmodia in the gall bladder wall. These two *Myxobolus* spp., together with myxospores of the genus *Ellipsomyxa*, were simultaneously observed in specimen #20. Specimens #12, #14, #18 and #19 displayed co-infection between *Ellipsomyxa* and the *Myxobolus* having bigger myxospores; specimen #17 displayed only the bigger myxospores of *Myxobolus*; and specimen #15 had only the smaller myxospores of *Myxobolus* (see Table 2). Apart from the gall bladder sample of specimen #20, all other samples were molecularly analysed and showed no evidence of co-infection between *Myxobolus*. The species having smaller myxospores is described here for the first time, while the species having bigger myxospores was identified as being *M. exiguus*. The myxospores of *Ellipsomyxa* were identified as belonging to the species *E. mugilis*.

Lastly, the infections detected in the spleen of specimens #13 and #18 were promptly regarded as co-infections, due to microscopic observations revealing the presence of two morphologically distinguishable morphotypes of *Myxobolus* (see Table 2).

In summary, regarding *C. ramada*, 7 *Myxobolus* spp. are described here: four from sites in which co-infection was registered, and three from sites of infection that were without microscopic or molecular evidence of co-infection. The latter included one species from the adipose tissue in the ocular cavity and urinary bladder; another from the pharyngobranchial organ in the opercular cavity; and the last from the skeletal and heart muscle (Figs. 1, 2, 3 and Table 3). Light photomicrographs and measurements are also provided for the unidentified *Myxobolus* morphotypes that appeared as co-infective in the gills, spleen, kidney and digestive tube (Fig. 4 and Table 4).

In the case of *C. labrosus*, one of the three specimens examined displayed macroscopic cysts attached to the visceral peritoneum, while the other two specimens displayed only plasmodia developing in the urinary bladder. Microscopic and molecular analyses showed no evidence of co-infection, so that both these species of *Myxobolus* are described here from *C. labrosus* (Fig. 5 and Table 3).

Regarding the myxozoan survey performed on *M. cephalus*, only infection by *Myxobolus* spp. was detected in five out of the 10 specimens examined. Infection was determined to occur in the gills, gall bladder, urinary bladder and intestine. Overall prevalence of infection was 30.0% in the gall bladder (3 infected in 10 specimens examined); 20.0% in the urinary bladder and intestine (2 infected in 10 specimens examined) and 10.0% in the gills (1 infected in 10 specimens examined). Microscopic and molecular analyses showed no evidence of co-infection between isolates of the same organ, but revealed significant differences among isolates of different organs, so that four *Myxobolus* species are described here from *M. cephalus* (Fig. 6 and Table 3).

Schematic drawings depicting the overall morphology of the myxospores in valvular view are provided for the 13 new *Myxobolus* spp. described herein (Fig. 7). Morphometric and biological data are summarized in Table 3, which further provides GenBank accession numbers and type material references for all the new species. Type material in the form of a series of phototypes and representative DNA samples of the hapantotypes was deposited in the Natural History and Science Museum of the University of Porto, Porto, Portugal.

Description of new species

Myxobolus ramadus n. sp.

Diagnosis: Cysts whitish and filamentous, about 2–3 mm in length, located in the gill lamellae. Myxospores spherical to subspherical in valvular view and ellipsoidal in sutural view, with two pyriform equally sized polar capsules located side by side at the anterior pole, and a small iodinophilous vacuole randomly located in the sporoplasm (Figs. 1a, b, 7a and Table 3).

Type host: The thinlip grey mullet *Chelon ramada* (Risso, 1827) (Teleostei, Mugilidae).

Type locality: The River Minho (41° 56′ N, 08° 45′ W), near "Vila Nova de Cerveira", Portugal.

Prevalence of infection: Four infected in 22 specimens examined (18.2%).

Material deposited: Series of phototypes of the hapantotype, deposited together with a representative DNA sample in the Natural History and Science Museum of the University of Porto, Portugal, reference CIIMAR 2019.27.

Etymology: The specific epithet "*ramadus*" refers to the host species.

Molecular data: One SSU rDNA gene sequence with a total of 2021 bp, representative of two identical sequences that

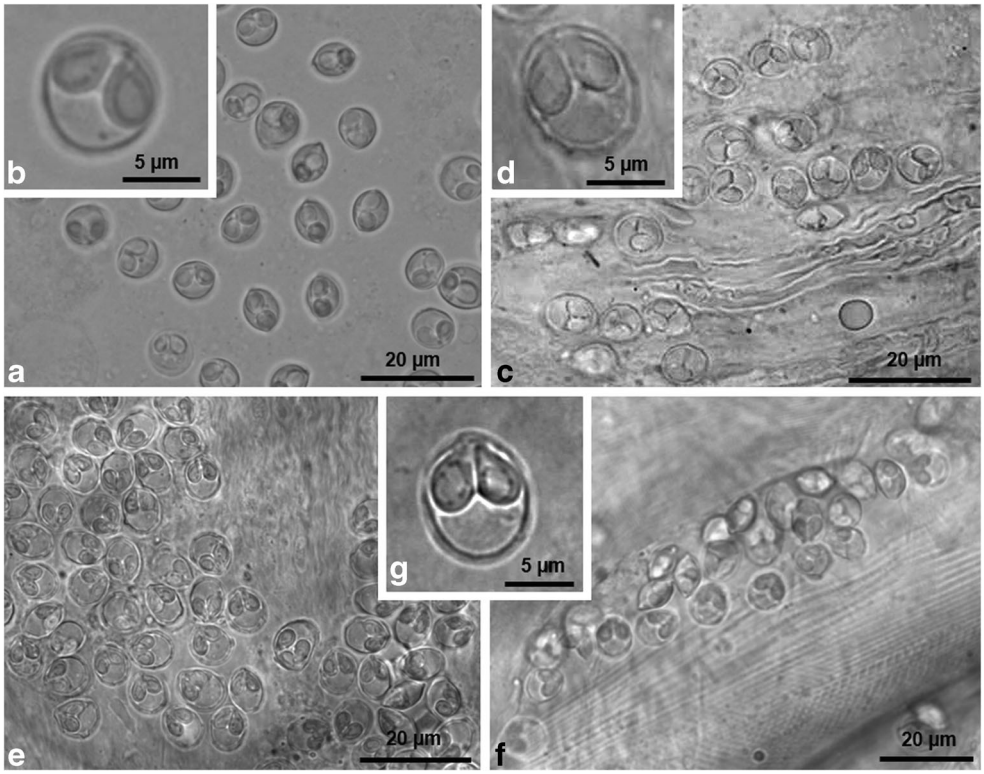

Fig. 1 Light micrographs of *Myxobolus* spp. infecting the thinlip grey mullet *Chelon ramada* in the River Minho. **a**–**b**. Myxospores of *M. ramadus* n. sp. as observed after rupture of a cyst in the gill lamellae. **c**–**d**. Myxospores of *M. pharyngobranchialis* n. sp. appearing disseminated in the denticulate pharyngeal pad of the pharyngobranchial organ, after rupture of a plasmodium. **e**–**g**. Myxospores of *M. muscularis* n. sp. as observed in the heart (**e**) and skeletal muscle (**f**), and in detail (**g**)

were separately assembled from the partial results obtained from macroscopic cysts in the gills of two infected specimens.

Remarks: Morphometry was determined from mature myxospores observed in all infected hosts. Individual measurements were identical between all case isolates, so no significant morphometric variation was recorded. Myxospores are morphologically similar to those of the unidentified *Myxobolus* sp. 3 in the spleen of this host, however,

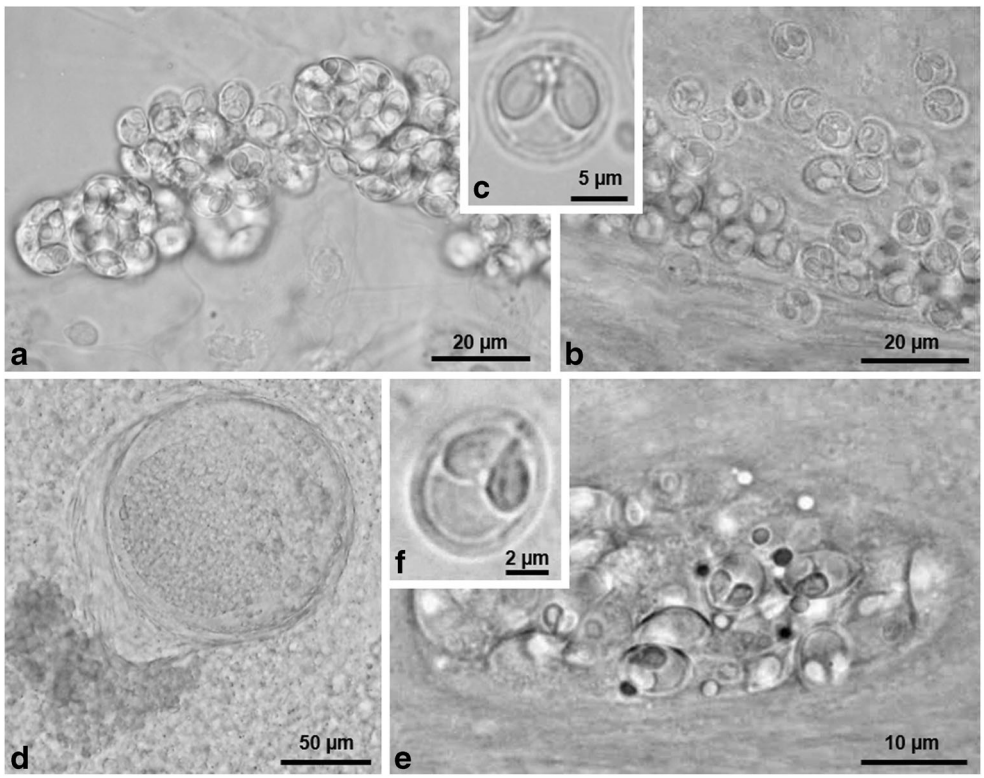

Fig. 2 Light micrographs of *Myxobolus* spp. infecting the thinlip grey mullet *Chelon ramada* in the River Minho. **a**–**c**. Myxospores of *M. adiposus* n. sp. forming clusters in the adipose tissue of the ocular cavity (**a**), appearing disseminated after rupture of a plasmodium in the urinary bladder (**b**), and as observed in detail (**c**). **d**–**f**. Myxospores of *M. hepatobiliaris* n. sp. forming microscopic cysts in the liver (**d**), developing in the gall bladder (**e**), and as observed in detail (**f**)

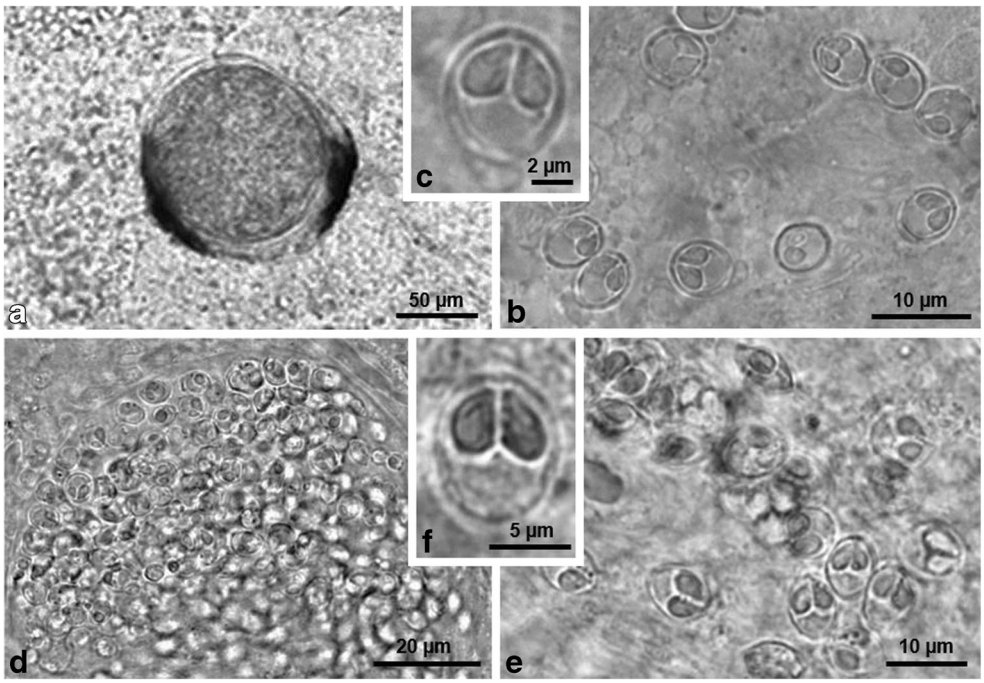

Fig. 3 Light micrographs of *Myxobolus* spp. infecting the thinlip grey mullet *Chelon ramada* in the River Minho. **a**–**c**. Myxospores of *M. renalis* n. sp. forming microscopic cysts in the kidney (**a**), appearing disseminated after rupture of a cyst (**b**), and as observed in detail (**c**). **d**–**f**. Myxospores of *M. cerveirensis* n. sp. forming plasmodia in the intestine (**d**), appearing disseminated after rupture of a plasmodium (**e**), and as observed in detail (**f**)

they differ in being significantly thicker (see Fig. 4 and Table 4). Comparison to all other *Myxobolus* spp. previously reported from mullet hosts revealed some morphometric similarity to *M. episquamalis*, *M. exiguus*, *Myxobolus hani* Faye et al., 1999 and *Myxobolus parsi* Das, 1996. The parasite in study, however, differs morphologically from all these species by lacking markings near its suture line. Moreover, the myxospores of *M. parsi* are bigger in terms of length and width, while those of *M. episquamalis* are narrower, being oval instead of subspherical or spherical (see Suppl. file S1; Egusa et al. 1990; Das 1996; Faye et al. 1999; Rocha et al. 2019a). Differentiation from *M. episquamalis* and *M. exiguus* is further ascertained by comparison of molecular data, given that distance estimation resulted in similarity values lower than 90.0% to all SSU rDNA sequences analysed, including *M. episquamalis* (88.8%) and *M. exiguus* (86.6%). Thus, this parasite is suggested as a new species, herein named *Myxobolus ramadus* n. sp.

Myxobolus pharyngobranchialis n. sp.

Diagnosis: Polysporic plasmodia located in the denticulate pharyngeal pad of the pharyngobranchial organ. Myxospores ellipsoidal in valvular and sutural view, with six to eight markings near the suture line. Two pyriform equally sized polar capsules located side by side at the anterior pole (Figs 1c, d, 7b and Table 3).

Type host: The thinlip grey mullet *Chelon ramada* (Risso, 1827) (Teleostei, Mugilidae).

Type locality: The River Minho (41° 56′ N, 08° 45′ W), near "Vila Nova de Cerveira", Portugal.

Prevalence of infection: Five infected in 22 specimens examined (22.7%).

Material Deposited: Series of phototypes of the hapantotype, deposited together with a representative DNA sample in the Natural History and Science Museum of the University of Porto, Portugal, reference CIIMAR 2019.28.

Etymology: The specific epithet "*pharyngobranchialis*" refers to the organ of infection in which the parasite was observed.

Molecular data: One SSU rDNA gene sequence with a total of 1993 bp, representative of five identical sequences that were separately assembled from the partial results obtained from plasmodia in the pharyngobranchial organ of five infected specimens.

Remarks: Morphometry was determined from mature myxospores observed in all infected hosts. Individual measurements were identical between all case isolates, so no significant morphometric variation was recorded. Myxospores are morphometrically similar to those of the unidentified *Myxobolus* sp. 3 from the spleen and *Myxobolus* sp. 4 from the kidney (see Fig. 4 and Table 4). The latter, however, differs by having oval myxospores that are significantly thinner and overall have longer polar capsules than those being described here. In turn, having the same shape and similar morphometric range, it is possible that the myxospores of the unidentified *Myxobolus* sp. 3 from the spleen belong to the parasite in study. Comparison to all other *Myxobolus* spp. previously reported from mullet hosts revealed some morphometric similarity to *M. episquamalis*, *M. exiguus*, *M. hani* and *Myxobolus* sp. of Kim et al. (2013b). Differentiation from both *M. hani* and *Myxobolus* sp. of Kim et al. (2013b) can be performed based on specific morphological traits: the myxospores of

Table 3 Host, site of infection, and morphometry of the myxospores of the new *Myxobolus* spp. described here from mullets in the River Minho, Portugal. SL: myxospore length; SW: myxospore width; ST: myxospore thickness; PCL: polar capsule length; PCW: polar capsule width; PTc: number of polar tubule coils. Measurements are means ± SD (range), given in μm. Type material deposited in the Natural History and Science Museum of the University of Porto, Portugal

Myxobolus spp.	Type host	Site of infection	SL	SW	ST	PCL	PCW	PTc	GenBank number	Type material
M. ramadus n. sp.	*C. ramada*	Gill lamellae	8.2 ± 0.5 (7.3–9.3) (*n* = 25)	7.9 ± 0.2 (7.3–8.3) (*n* = 25)	6.4 ± 0.2 (6.0–6.7) (*n* = 25)	4.2 ± 0.2 (4.0–4.3) (*n* = 25)	3.0 ± 0.3 (2.7–3.3) (*n* = 25)	5–6	MK203074	CIIMAR 2019.27
M. pharyngobranchialis n. sp.	*C. ramada*	Pharyngobranchial organ	9.3 ± 0.4 (8.7–10.0) (*n* = 50)	7.7 ± 0.4 (7.0–8.0) (*n* = 50)	5.8 ± 0.5 (4.7–6.0) (*n* = 8)	4.7 ± 0.3 (4.0–5.3) (*n* = 50)	2.9 ± 0.2 (2.7–3.3) (*n* = 50)	6–7	MK203073	CIIMAR 2019.28
M. muscularis n. sp.	*C. ramada*	Skeletal and heart muscle	9.1 ± 0.6 (8.0–10.0) (*n* = 50)	7.0 ± 0.6 (6.0–8.7) (*n* = 50)	5.2 ± 0.3 (4.7–6.0) (*n* = 30)	4.3 ± 0.3 (4.0–5.0) (*n* = 50)	2.7 ± 0.2 (2.0–3.3) (*n* = 50)	5–6	MK203075	CIIMAR 2019.29
M. adiposus n. sp.	*C. ramada*	The adipose tissue	9.1 ± 0.3 (8.7–9.3) (*n* = 55)	9.0 ± 0.3 (8.7–9.3) (*n* = 55)	–	4.6 ± 0.3 (4.0–5.3) (*n* = 55)	3.0 ± 0.3 (2.7–3.3) (*n* = 55)	6–7	MK203076	CIIMAR 2019.30
M. hepatobiliaris n. sp.	*C. ramada*	Liver and gall bladder	6.6 ± 0.3 (6.0–7.0) (*n* = 47)	5.2 ± 0.3 (4.7–5.7) (*n* = 47)	4.1 ± 0.2 (4.0–4.3) (*n* = 26)	3.0 ± 0.2 (2.7–3.3) (*n* = 50)	1.7 ± 0.2 (1.7–2.0) (*n* = 50)	4	MK203078	CIIMAR 2019.31
M. renalis n. sp.	*C. ramada*	Kidney	6.7 ± 0.2 (6.3–7.3) (*n* = 40)	5.8 ± 0.2 (5.3–6.0) (*n* = 40)	4.6 ± 0.2 (4.3–5.0) (*n* = 17)	3.1 ± 0.2 (2.7–3.7) (*n* = 40)	1.9 ± 0.2 (1.7–2.3) (*n* = 40)	4	MK203077	CIIMAR 2019.32
M. cerveirensis n. sp.	*C. ramada*	Intestine	8.1 ± 0.2 (7.7–8.7) (*n* = 25)	6.8 ± 0.2 (6.7–7.3) (*n* = 25)	5.3 ± 0.3 (5.0–5.7) (*n* = 4)	4.2 ± 0.2 (4.0–4.7) (*n* = 25)	2.8 ± 0.2 (2.3–3.0) (*n* = 25)	4–5	MK203079	CIIMAR 2019.33
M. peritonaeum n. sp.	*C. labrosus*	Visceral peritoneum	8.1 ± 0.2 (8.0–8.3) (*n* = 25)	7.1 ± 0.2 (6.7–7.3) (*n* = 25)	–	3.8 ± 0.2 (3.3–4.0) (*n* = 25)	2.4 ± 0.2 (2.0–2.7) (*n* = 25)	4–5	MK203080	CIIMAR 2019.34
M. labrosus n. sp.	*C. labrosus*	Urinary bladder	10.0 ± 0.2 (9.7–10.3) (*n* = 25)	8.1 ± 0.3 (7.7–8.7) (*n* = 25)	5.8 ± 0.2 (5.7–6.0) (*n* = 25)	4.5 ± 0.2 (4.0–5.0) (*n* = 25)	2.5 ± 0.2 (2.3–2.7) (*n* = 25)	5–7	MK203081	CIIMAR 2019.35
M. mugiliensis n. sp.	*M. cephalus*	Gill lamellae	11.4 ± 0.2 (11.0–11.7) (*n* = 25)	9.6 ± 0.4 (9.0–10.3) (*n* = 25)	6.5 ± 0.2 (6.0–6.7) (*n* = 25)	4.9 ± 0.2 (4.7–5.3) (*n* = 25)	3.0 ± 0.2 (2.7–3.3) (*n* = 25)	5	MK203082	CIIMAR 2019.36
M. vesicularis n. sp.	*M. cephalus*	Connective tissue	11.9 ± 0.4 (11.3–12.7) (*n* = 25)	10.3 ± 0.2 (10.0–10.7) (*n* = 25)	6.8 ± 0.3 (6.3–7.0) (*n* = 5)	4.9 ± 0.2 (4.7–5.3) (*n* = 25)	3.1 ± 0.2 (2.7–3.3) (*n* = 25)	4–5	MK203085	CIIMAR 2019.37
M. urinaris n. sp.	*M. cephalus*	Urinary bladder	10.0 ± 0.3 (9.3–10.3) (*n* = 23)	8.2 ± 0.3 (7.7–8.7) (*n* = 23)	–	4.0 ± 0.3 (3.3–4.7) (*n* = 25)	2.8 ± 0.1 (2.7–3.0) (*n* = 25)	4–5	MK203083	CIIMAR 2019.38
M. galaicoportucalensis n. sp.	*M. cephalus*	Intestine	11.9 ± 0.4 (11.3–12.7) (*n* = 75)	10.2 ± 0.2 (10.0–10.7) (*n* = 75)	6.7 ± 0.2 (6.0–7.0) (*n* = 27)	4.7 ± 0.3 (4.0–5.3) (*n* = 76)	2.9 ± 0.2 (2.7–3.3) (*n* = 76)	4–5	MK203084	CIIMAR 2019.39

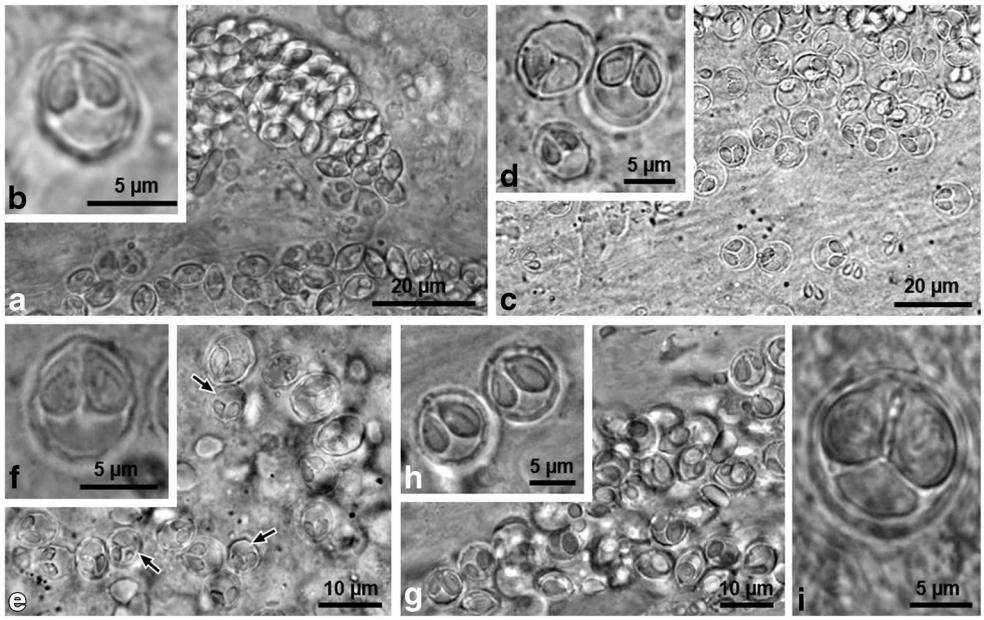

Fig. 4 Light micrographs of the unidentified *Myxobolus* spp. infecting the thinlip grey mullet *Chelon ramada* in the River Minho. **a**–**b**. Myxospores of *Myxobolus* sp. 1 as observed after rupture of a microscopic cyst in the afferent artery of the gill filaments (**a**), and in detail (**b**). **c**–**d**. Myxospores of *Myxobolus* sp. 2 (smaller) and *Myxobolus* sp. 3 (bigger) appearing disseminated among each other in the spleen. **e**–**f**. Myxospores of *Myxobolus* sp. 4 disseminated in the kidney after rupture of a plasmodium. Notice the presence of the smaller myxospores of *M. renalis* n. sp. (arrows) among those of *Myxobolus* sp. 4. **g**–**h**. Myxospores of *Myxobolus* sp. 5 as observed after rupture of a plasmodium located in the intestinal wall. **i**. Myxospore of *Myxobolus* sp. 6 as observed disseminated in the intestinal wall

M. hani are significantly shorter and have a subspherical shape, rather than the ellipsoidal shape reported here, while those of *Myxobolus* sp. of Kim et al. (2013b) are larger with smaller polar capsules (see Suppl. file S1; Faye et al. 1999). In turn, differentiation from *M. episquamalis* and *M. exiguus* is mainly based on the molecular comparison of SSU rDNA sequences, considering that few distinctive morphological traits exist between these species and the parasite being described. Overall, the myxospores of *M. episquamalis* differ from those in study only in their oval shape, while those of *M. exiguus* display a higher number of polar tubule coils and fewer number of sutural markings. Distance estimation resulted in similarity values lower than 96.0% to all SSU rDNA sequences analysed, including *M. episquamalis* (86.9%), *M. exiguus* (92.6%) and *Myxobolus* sp. of Kim et al. (2013b) (86.0%). Thus, this parasite is suggested as a new species, herein named *Myxobolus pharyngobranchialis* n. sp.

Myxobolus muscularis n. sp.

Diagnosis: Polysporic plasmodia located in the fibres of the heart (Fig. 1e) and skeletal muscle (Fig. 1f). Myxospores oval in valvular view and ellipsoidal in sutural view, displaying 8 to 10 markings surrounding the posterior half of the suture line. Two pyriform equally sized polar capsules located side by side at the anterior pole (Figs. 1g, 7c and Table 3).

Type host: The thinlip grey mullet *Chelon ramada* (Risso, 1827) (Teleostei, Mugilidae).

Type locality: The River Minho (41° 56′ N, 08° 45′ W), near "Vila Nova de Cerveira", Portugal.

Prevalence of infection: Three infected in 22 specimens examined (13.6%): two specimens with infection in the heart (9.1%), and two with infection in the skeletal muscle (9.1%), meaning that one of the three specimens displayed infection by this species in both the skeletal and heart muscle.

Material Deposited: Series of phototypes of the hapantotype, deposited together with a representative DNA sample in the Natural History and Science Museum of the University of Porto, Portugal, reference CIIMAR 2019.29.

Etymology: The specific epithet "*muscularis*" refers to the site of infection of the parasite.

Molecular data: One SSU rDNA gene sequence with a total of 2009 bp, representative of four identical sequences that were separately assembled from the partial results obtained from plasmodia in four tissue samples (two from the heart muscle, and the other two from the skeletal muscle), belonging to a total of three infected specimens.

Remarks: Morphometry was determined from mature myxospores observed in both infected hosts. Individual measurements were identical between both case isolates, so no significant morphometric variation was recorded. Myxospores display some morphometric similarity to the unidentified *Myxobolus* sp. 3 from the spleen and the unidentified *Myxobolus* sp. 4 from the kidney (see Fig. 4 and Table 4), however, differing in significant morphological traits. The

Table 4 Site of infection and morphometry of the unidentified *Myxobolus* myxospores observed in the thinlip grey mullet *Chelon ramada* from the River Minho, Portugal. SL: myxospore length; SW: myxospore width; ST: myxospore thickness; PCL: polar capsule length; PCW: polar capsule width; PTc: number of polar tubule coils; L: larger; S: smaller. Measurements are means ± SD (range), given in μm.

Myxobolus spp.	Site of infection	SL	SW	ST	PCL	PCW	PTc
Myxobolus sp. 1	Gill filaments	6.9 ± 0.3 (6.3–7.3) (*n* = 40)	5.9 ± 0.5 (4.7–6.7) (*n* = 40)	4.2 ± 0.2 (4.0–4.7) (*n* = 40)	3.1 ± 0.2 (2.7–3.3) (*n* = 45)	1.8 ± 0.2 (1.3–2.0) (*n* = 45)	–
Myxobolus sp. 2	Spleen	7.1 ± 0.4 (6.5–8.0) (*n* = 25)	5.5 ± 0.3 (5.1–6.0) (*n* = 25)	4.3 ± 0.3 (3.8–4.7) (*n* = 21)	3.1 ± 0.3 (2.6–3.6) (*n* = 25)	2.1 ± 0.2 (1.6–2.4) (*n* = 25)	3–4
Myxobolus sp. 3	Spleen	8.9 ± 0.4 (7.9–9.6) (*n* = 25)	7.9 ± 0.4 (7.1–8.5) (*n* = 25)	5.5 ± 0.3 (5.2–6.1) (*n* = 9)	4.5 ± 0.2 (4.0–5.0) (*n* = 25)	2.7 ± 0.2 (2.5–3.2) (*n* = 25)	6
Myxobolus sp. 4	Kidney	9.6 ± 0.3 (9.0–10.0) (*n* = 30)	6.7 ± 0.3 (6.3–7.3) (*n* = 30)	5.5 ± 0.2 (5.3–6.0) (*n* = 8)	4.9 ± 0.2 (4.7–5.3) (*n* = 50)	3.0 ± 0.2 (2.7–3.3) (*n* = 50)	5–6
Myxobolus sp. 5	Intestine	7.8 ± 0.4 (7.2–8.8) (*n* = 30)	7.5 ± 0.4 (6.5–8.5) (*n* = 30)	5.5 ± 0.3 (5.1–6.0) (*n* = 26)	L 4.7 ± 0.4 (3.9–5.4) (*n* = 25) S 3.6 ± 0.2 (3.3–4.2) (*n* = 25)	L 3.3 ± 0.2 (3.0–3.8) (*n* = 25) S 2.1 ± 0.2 (1.6–2.4) (*n* = 25)	L 8 S 6
Myxobolus sp. 6	Intestine	15.0 ± 0.4 (14.7–15.7) (*n* = 8)	13.7 ± 0.4 (13.3–14.7) (*n* = 8)	–	7.9 ± 0.5 (6.7–8.7) (*n* = 16)	5.3 ± 0.4 (4.7–6.0) (*n* = 16)	–

myxospores of the unidentified *Myxobolus* sp. 3 from the spleen are ellipsoidal instead of oval, while those of the unidentified *Myxobolus* sp. 4 from the kidney are more elongated with bigger polar capsules. Comparison to all other *Myxobolus* spp. previously reported from mullet hosts revealed the parasite displaying some morphological similarity with *Myxobolus anili* Sarkar, 1989, *Myxobolus cheni* Schulman, 1962, *M. episquamalis*, *M. exiguus*, *M. hani* and *M. parsi*. The myxospores of *M. anili*, *M. exiguus* and *M. hani*, however, differ from those in study in terms of shape (*M. anili* is ellipsoidal, while both *M. exiguus* and *M. hani* are subspherical). Moreover, the myxospores of *M. anili* are significantly longer and larger, while those of *M. parsi* are much thicker, with their length and width falling close to the superior limit of the morphometric range reported here. On the other way around, *M. cheni* has a smaller morphometric range that overlaps with that of the parasite in study at its inferior limit; therefore, the myxospores of *M. cheni* are generally smaller than those being described here. Overall, highest resemblance was found in relation to *M. episquamalis*, if considered that it shares the same oval shape, markings near the suture line, and morphometric range (see Suppl. file S1). Differentiation from this species was only possible through the molecular comparison of SSU rDNA sequences. Distance estimation resulted in similarity values lower than 95.0% to all SSU rDNA sequences analysed, including *M. exiguus* (90.7%) and *M. episquamalis* (88.7%). Thus, this parasite is suggested as a new species, herein named *Myxobolus muscularis* n. sp.

Myxobolus adiposus n. sp.

Diagnosis: Clusters of myxospores forming plasmodia attached to the adipose tissue surrounding the optic nerve in the ocular cavity (Fig. 2a), and in the urinary bladder (Fig. 2b). Myxospores spherical, displaying 12 to 14 markings near the suture line. Two pyriform equally sized polar capsules located side by side at the anterior pole (Figs. 2c, 7d and Table 3).

Type host: The thinlip grey mullet *Chelon ramada* (Risso, 1827) (Teleostei, Mugilidae).

Other hosts: The flathead grey mullet *Mugil cephalus* Linnaeus, 1758 (Teleostei, Mugilidae).

Type locality: The River Minho (41° 56′ N, 08° 45′ W), near "Vila Nova de Cerveira", Portugal.

Other localities: The Mediterranean Sea off Northern Israel.

Prevalence of infection: Five infected in 22 specimens examined (22.7%): five specimens with infection in the ocular cavity (22.7%), two of which also displaying infection in the urinary bladder (18.2%).

Material deposited: Series of phototypes of the hapantotype, deposited together with a representative DNA sample in the Natural History and Science Museum of the University of Porto, Portugal, reference CIIMAR 2019.30.

Etymology: The specific epithet "*adiposus*" refers to the site of infection of the parasite being the adipose tissue.

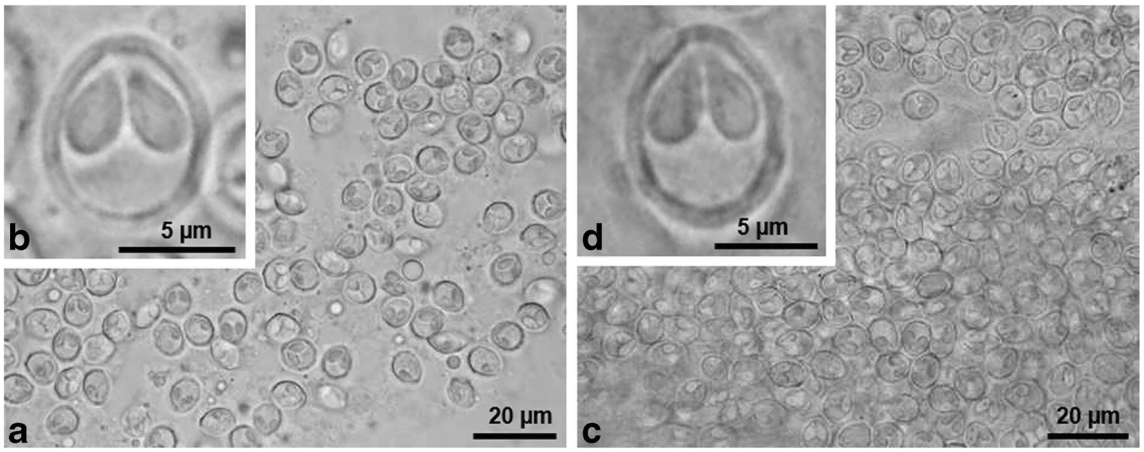

Fig. 5 Light micrographs of *Myxobolus* spp. infecting the thicklip grey mullet *Chelon labrosus* in the River Minho. **a**–**b**. Myxospores of *M. peritonaeum* n. sp. as observed after rupture of a macroscopic cyst attached to the visceral peritoneum. **c**–**d**. Myxospores of *M. labrosus* n. sp. forming plasmodia in the urinary bladder (**c**), and as observed in detail (**d**)

Molecular data: One SSU rDNA gene sequence with a total of 2000 bp, representative of seven identical sequences that were separately assembled from the partial results obtained from plasmodia in seven samples of adipose tissue (five from the ocular cavity, and the other two from the urinary bladder), belonging to a total of five infected specimens.

Remarks: Morphometry was determined from mature myxospores observed in all infected hosts. Individual measurements were identical between case isolates, so no significant morphometric variation was recorded. Having spherical myxospores, this parasite differs significantly from all others reported here. In the same manner, no significant similarity was found in relation to all other *Myxobolus* spp. morphologically reported from mullet hosts (see Suppl. file S1). Distance estimation, however, revealed 99.8% of similarity to the SSU rDNA sequence of a *Myxobolus* sp. (MF118765) that was recently reported from infections in the gills, intestine, and tail of *M. cephalus* from the Mediterranean Sea off Northern Israel (isolate IsraelMS gipt) (Sharon et al. 2019), and this small divergence led us to consider them as being of the same species. All other SSU rDNA sequences included in the analysis showed similarity values lower than 95.0% to the parasite in

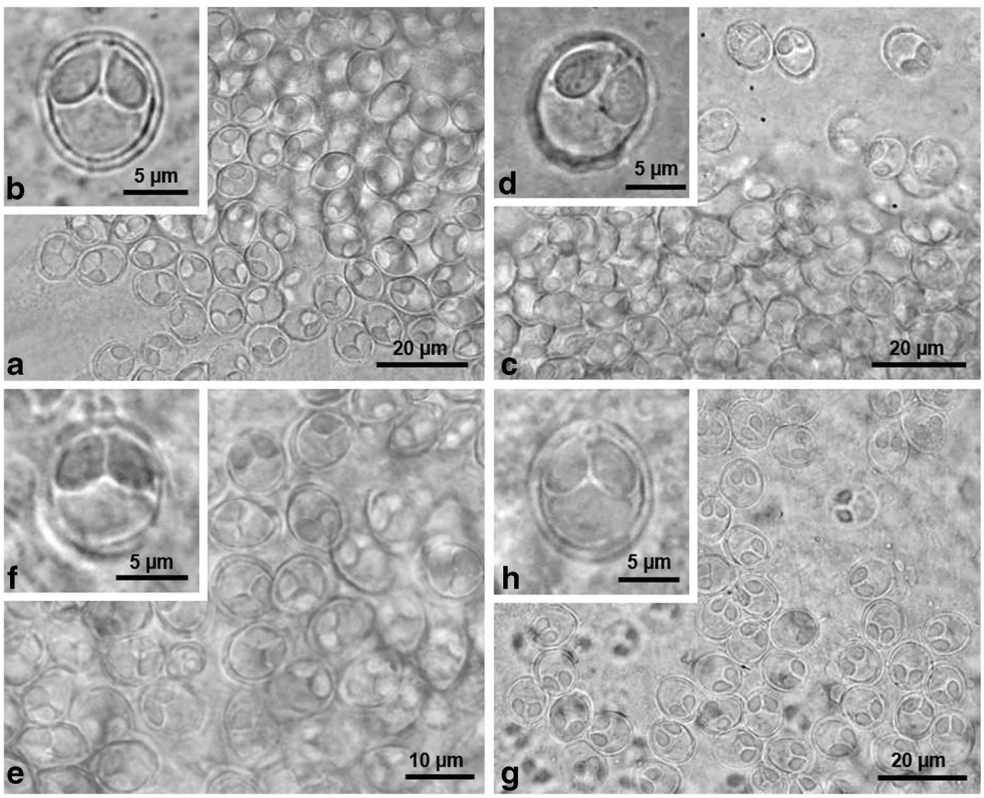

Fig. 6 Light micrographs of *Myxobolus* spp. infecting the flathead grey mullet *Mugil cephalus* in the River Minho. **a**–**b**. Myxospores of *M. mugiliensis* n. sp. as observed after rupture of a macroscopic cyst in the gill lamellae (**a**), and in detail (**b**). **c**–**d**. Myxospores of *M. vesicularis* n. sp. forming plasmodia in the gall bladder wall (**c**), and as observed in detail (**d**). **e**–**f**. Myxospores of *M. urinaris* n. sp. forming plasmodia in the urinary bladder wall (**e**), and as observed in detail (**f**). **g**–**h**. Myxospores of *M. galaicoportucalensis* n. sp. appearing disseminated after rupture of a plasmodium in the intestinal wall (**g**), and as observed in detail (**h**).

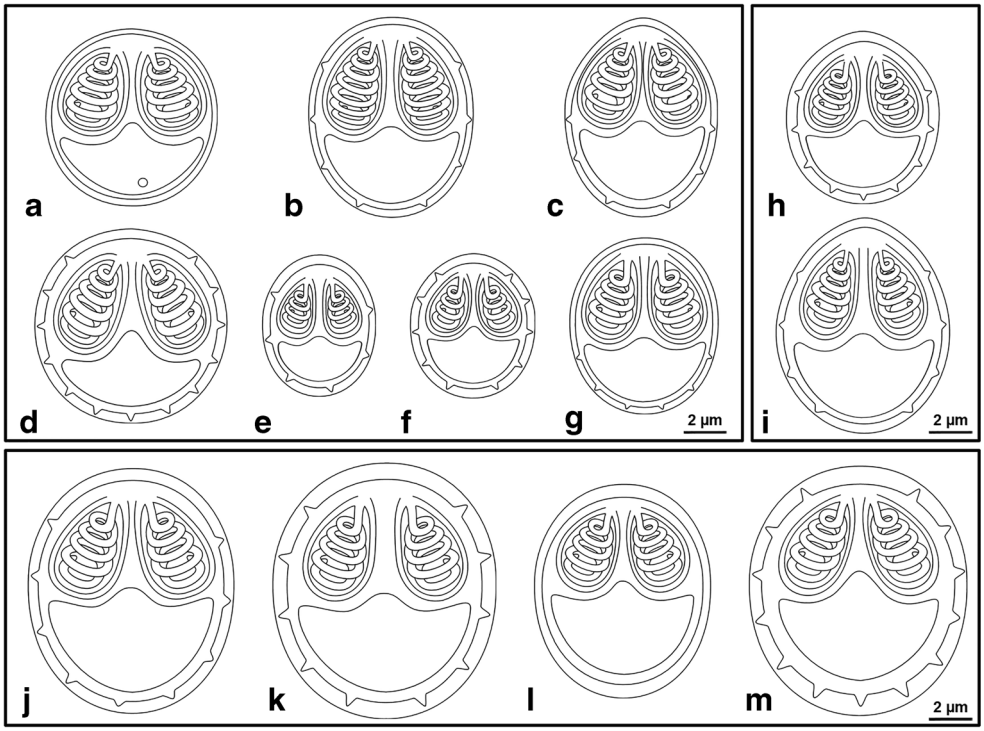

Fig. 7 Schematic drawings of the myxospores of the 13 new *Myxobolus* spp. described here from mullets in the River Minho, as observed in valvular view. **a**. *M. ramadus* n. sp. **b**. *M. pharyngobranchialis* n. sp. **c**. *M. muscularis* n. sp. **d**. *M. adiposus* n. sp. **e**. *M. hepatobiliaris* n. sp. **f**. *M. renalis* n. sp. **g**. *M. cerveirensis* n. sp. **h**. *M. peritonaeum* n. sp. **i**. *M. labrosus* n. sp. **j**. *M. mugiliensis* n. sp. **k**. *M. vesicularis* n. sp. **l**. *M. urinaris* n. sp. **m**. *M. galaicoportucalensis* n. sp

study. Considering all the above, this parasite is suggested as a new species, herein named *Myxobolus adiposus* n. sp., with *C. ramada* as type host and the River Minho as type locality. Other hosts, sites of infection and geographic localities are included in the summary provided as supplementary material (see Suppl. file S1).

Myxobolus hepatobiliaris n. sp.

Diagnosis: Microscopic cysts in the liver (Fig. 2d) and gall bladder wall (Fig. 2e). Myxospores ellipsoidal in valvular and sutural view, displaying six to eight markings near the suture line. Two pyriform equally sized polar capsules located side by side at the anterior pole (Figs. 2f, 7e and Table 3).

Type host: The thinlip grey mullet *Chelon ramada* (Risso, 1827) (Teleostei, Mugilidae).

Type locality: The River Minho (41° 56′ N, 08° 45′ W), near "Vila Nova de Cerveira", Portugal.

Prevalence of infection: Two infected in 22 specimens examined (9.1%): one specimen with infection in the liver (4.5%), and another with infection in the gall bladder wall (4.5%).

Material deposited: Series of phototypes of the hapantotype, deposited together with a representative DNA sample in the Natural History and Science Museum of the University of Porto, Portugal, reference CIIMAR 2019.31.

Etymology: The specific epithet "*hepatobiliaris*" refers to the organs of infection in which the parasite was observed.

Molecular data: One SSU rDNA gene sequence with a total of 1962 bp, representative of two identical sequences that were separately assembled from the partial results obtained from microscopic cysts in two tissue samples (one from the liver, and another from the gall bladder), belonging to a total of two infected specimens.

Remarks: Morphometry was determined from mature myxospores observed in both infected hosts. Individual measurements were identical between case isolates, so no significant morphometric variation was recorded. Myxospores are morphometrically similar to those of the unidentified *Myxobolus* sp. 1 from the gills, with slighter resemblance to those of the unidentified *Myxobolus* sp. 2 from the spleen (see Fig. 4 and Table 4). Nonetheless, the myxospores of the latter differ in being overall bigger, while the myxospores of the unidentified *Myxobolus* sp. 1 from the gills are oval shaped instead of ellipsoidal, moreover being generally larger than those described here. Comparison to all other *Myxobolus* spp. previously reported from mullet hosts revealed some morphometric similarity to *Myxobolus macrolepi* Dorothy and Kalavati, 1992, *Myxobolus mugauratus* (Pogoreltseva, 1964) Landsberg and Lom, 1991 and *Myxobolus parvus* Schulman, 1962. The myxospores of *M. macrolepi*, however, have a significantly wider morphometric range and higher number of polar tubule coils (six to seven against the four reported here), while those of both *M. mugauratus* and *M. parvus* have notably bigger polar capsules. The myxospores of *M. parvus* are also larger than those of the parasite in study (see Suppl. file S1). Distance estimation showed a high similarity to the *Myxobolus* species described here from the kidney of *C. ramada* (97.3%), with all other SSU rDNA sequences included in the analysis resulting in

similarity values lower than 92.0%, including *M. parvus* (89.3%). Thus, this parasite is suggested as a new species, herein named *Myxobolus hepatobiliaris* n. sp.

Myxobolus renalis n. sp.

Diagnosis: Microscopic cysts developing in the kidney (Fig. 3a). Myxospores ellipsoidal to subspherical in valvular view and ellipsoidal in sutural view, displaying 8 to 10 markings near the suture line. Two pyriform equally sized polar capsules located side by side at the anterior pole (Figs. 3b, c, 7f and Table 3).

Type host: The thinlip grey mullet *Chelon ramada* (Risso, 1827) (Teleostei, Mugilidae).

Type locality: The River Minho (41° 56′ N, 08° 45′ W), near "Vila Nova de Cerveira", Portugal.

Prevalence of infection: Three specimens molecularly confirmed to be infected by this parasite in 22 specimens examined (13.6%).

Material deposited: Series of phototypes of the hapantotype, deposited together with a representative DNA sample in the Natural History and Science Museum of the University of Porto, Portugal, reference CIIMAR 2019.32.

Etymology: The specific epithet "*renalis*" refers to the organ of infection in which the parasite was observed.

Molecular data: One SSU rDNA gene sequence with a total of 1976 bp, representative of three identical sequences that were separately assembled from the partial results obtained from microscopic cysts in kidney samples of three infected specimens.

Remarks: Morphometry was determined from mature myxospores observed in the three host specimens molecularly confirmed to be infected by this parasite. Individual measurements were identical between case isolates, so no significant morphometric variation was recorded. Myxospores are morphometrically similar to those of the unidentified *Myxobolus* sp. 2 from the spleen of *C. ramada* (see Fig. 4 and Table 4), and possibly belong to the same species, despite the myxospores in the spleen being overall more elongated than those described here. Although some morphometric similarity could also be found in relation to the unidentified *Myxobolus* sp. 1 from the gills (see Fig. 4 and Table 4), the myxospores of the latter differ in being oval shaped instead of ellipsoidal to subspherical. Comparison to all other *Myxobolus* spp. previously reported from mullet hosts revealed some morphometric similarity to *M. macrolepi*, *M. parvus* and *Myxobolus supamattayai* U-taynapun et al., 2011. The parasite in study differs from *M. macrolepi* in having myxospores with stricter morphometric range and fewer number of polar tubule coils (4 against the 6 to 7 turns of *M. macrolepi*). In turn, the myxospores of *M. parvus* have longer polar capsules than those in study, while *M. supamattayai* myxospores are larger (see Suppl. file S1). Differentiation of the parasite in study from these two latter species, however, is mainly based on the molecular comparison of SSU rDNA sequences. Distance estimation showed a high similarity to the *Myxobolus* species described here from the liver and gall bladder of *C. ramada* (97.3%), with all other SSU rDNA sequences analysed resulting in similarity values lower than 92.0%, including *M. parvus* (89.7%) and *M. supamattayai* (84.1%). Thus, this parasite is suggested as a new species, herein named *Myxobolus renalis* n. sp.

Myxobolus cerveirensis n. sp.

Diagnosis: Polysporic plasmodia located in the intestine (Fig. 3d). Myxospores ellipsoidal in valvular and sutural view, with at least six markings surrounding the posterior half of the suture line. Two pyriform equally sized polar capsules located side by side at the anterior pole (Figs. 3e, f, 7g and Table 3).

Type host: The thinlip grey mullet *Chelon ramada* (Risso, 1827) (Teleostei, Mugilidae).

Type locality: The River Minho (41° 56′ N, 08° 45′ W), near "Vila Nova de Cerveira", Portugal.

Prevalence of infection: One specimen molecularly confirmed to be infected by this parasite in 22 specimens examined (4.5%).

Material deposited: Series of phototypes of the hapantotype, deposited together with a representative DNA sample in the Natural History and Science Museum of the University of Porto, Portugal, reference CIIMAR 2019.33.

Etymology: The specific epithet "*cerveirensis*" refers to the type locality of the parasite in the River Minho, which is near "Vila Nova de Cerveira".

Molecular data: One SSU rDNA gene sequence with a total of 1976 bp, assembled from the identical partial sequences obtained from plasmodia in the intestine of a single specimen.

Remarks: Morphometry was determined from mature myxospores observed in a single infected host. Myxospores without significant overall morphometric similarity to the unidentified species reported here from *C. ramada*. Comparison to all other *Myxobolus* spp. previously reported from mullet hosts revealed some morphometric similarity to *M. episquamalis* and *M. hani*. The myxospores of the latter can be differentiated from those in study by their subspherical shape and larger width. In turn, the myxospores of *M. episquamalis* differ only in their oval shape, considering that the measurements of the parasite in study are well within the morphometric range reported for this species (see Suppl. file S1; Egusa et al. 1990; Faye et al. 1999). Despite the morphological likeness, distance estimation showed low similarity to *M. episquamalis* (86.7%), as well as to all other SSU rDNA sequences analysed, which did not surpass 92.0% of similarity. Thus, this parasite is suggested as a new species, herein named *Myxobolus cerveirensis* n. sp.

Myxobolus peritonaeum n. sp.

Diagnosis: Cysts yellowish, subspherical to filamentous, and measuring about 1–2 mm, attached to the visceral peritoneum. Myxospores oval in valvular view, displaying 8 to 10 markings near the suture line. Two pyriform equally sized

polar capsules located side by side at the anterior pole (Figs. 5a, b, 7h and Table 3).

Type host: The thicklip grey mullet *Chelon labrosus* (Risso, 1827) (Teleostei, Mugilidae).

Type locality: The River Minho (41° 56′ N, 08° 45′ W), near "Vila Nova de Cerveira", Portugal.

Prevalence of infection: One infected in three specimens examined (33.3%).

Material deposited: Series of phototypes of the hapantotype, deposited together with a representative DNA sample in the Natural History and Science Museum of the University of Porto, Portugal, reference CIIMAR 2019.34.

Etymology: The specific epithet "*peritonaeum*" refers to the site of infection of the parasite.

Molecular data: One SSU rDNA gene sequence with a total of 1976 bp, assembled from the identical partial sequences obtained from cysts excised from the visceral peritoneum of a single infected specimen.

Remarks: Morphometry was determined from mature myxospores observed in cysts collected from a single infected host. Comparison to all other *Myxobolus* spp. previously reported from mullet hosts revealed the parasite in study having high morphological similarity to *M. episquamalis*. Although *M. exiguus* and *M. mugchelo* have also been found in the peritoneum of *C. labrosus*, the myxospores in study are overall smaller than those of *M. exiguus*, while being larger than those of *M. mugchelo* (see Suppl. file S1). Despite the morphological likeness to *M. episquamalis*, distance estimation showed low similarity to this species (88.0%), as well as to all other SSU rDNA sequences analysed, which did not surpass 96.0% of similarity. Thus, this parasite is suggested as a new species, herein named *Myxobolus peritonaeum* n. sp.

Myxobolus labrosus n. sp.

Diagnosis: Polysporic plasmodia located in the urinary bladder. Myxospores oval in valvular view and ellipsoidal in sutural view, displaying about eight markings near the suture line. Two pyriform equally sized polar capsules located side by side at the slightly pointed anterior pole (Figs. 5c, d, 7i and Table 3).

Type host: The thicklip grey mullet *Chelon labrosus* (Risso, 1827) (Teleostei, Mugilidae).

Type locality: The River Minho (41° 56′ N, 08° 45′ W), near "Vila Nova de Cerveira", Portugal.

Prevalence of infection: Two infected in three specimens examined (66.7%).

Material deposited: Series of phototypes of the hapantotype, deposited together with a representative DNA sample in the Natural History and Science Museum of the University of Porto, Portugal, reference CIIMAR 2019.35.

Etymology: The specific epithet "*labrosus*" refers to the specific epithet of the host species.

Molecular data: One SSU rDNA gene sequence with a total of 1965 bp, representative of two identical sequences that were separately assembled from the partial results obtained from plasmodia in the urinary bladder samples of two infected specimens.

Remarks: Morphometry was determined from mature myxospores observed in both infected hosts. Individual measurements were identical between case isolates, so no significant morphometric variation was recorded. Comparison to all other *Myxobolus* spp. previously reported from mullet hosts revealed some morphometric similarity to *M. anili*, *Myxobolus bankimi* Sarkar, 1999, *M. exiguus*, and *Myxobolus* sp. of Kim et al. (2013b) (see Suppl. file S1). Morphological differentiation between the parasite in study and most of the above-mentioned species is mainly based on their myxospores' shape not being oval [*M. exiguus* myxospores are subspherical, while those of *M. anili* and *Myxobolus* sp. of Kim et al. (2013b) are ellipsoidal] (see Sarkar 1989; Kim et al. 2013b; Rocha et al. 2019a). Only *M. bankimi* was described to have ovoid to elongated ovoid shaped myxospores that closely resemble those reported here (see Sarkar 1999). Nonetheless, the myxospores of the latter species are generally longer with shorter polar capsules, additionally lacking the sutural markings that characterize the myxospores of the parasite in study (see Suppl. file S1). Differentiation from *M. exiguus* and *Myxobolus* sp. of Kim et al. (2013b) was further ascertained through molecular comparison of respective SSU rDNA sequences. Distance estimation showed low similarity to *M. exiguus* (93.2%) and *Myxobolus* sp. of Kim et al. (2013b) (86.0%), as well as to all other SSU rDNA sequences analysed, which did not surpass 96.0% of similarity. Thus, this parasite is suggested as a new species, herein named *Myxobolus labrosus* n. sp.

Myxobolus mugiliensis n. sp.

Diagnosis: Cysts whitish, subspherical to filamentous, about 1–2 mm in length, located in the gill lamellae. Myxospores ellipsoidal in valvular and sutural view, displaying 8 to 10 markings near the suture line. Two pyriform equally sized polar capsules located side by side at the anterior pole (Figs. 6a, b, 7j and Table 3).

Type host: The flathead grey mullet *Mugil cephalus* Linnaeus, 1758 (Teleostei, Mugilidae).

Type locality: The River Minho (41° 56′ N, 08° 45′ W), near "Vila Nova de Cerveira", Portugal.

Other localities: The Spanish Mediterranean coast, and possibly the Samsun coasts of the Black Sea in Turkey.

Prevalence of infection: One infected in ten specimens examined (10.0%).

Material deposited: Series of phototypes of the hapantotype, deposited together with a representative DNA sample in the Natural History and Science Museum of the University of Porto, Portugal, reference CIIMAR 2019.36.

Etymology: The specific epithet "*mugiliensis*" refers to the name of the genus of the host species.

Molecular data: One SSU rDNA gene sequence with a total of 1972 bp, assembled from the identical partial sequences obtained from cysts excised from the gills of a single infected specimen.

Remarks: Morphometry was determined from mature myxospores observed in cysts collected from a single infected host. Comparison to all other *Myxobolus* spp. previously reported from mullet hosts revealed significant similarity to *M. rohdei*, *Myxobolus spinacurvatura* Maeno et al., 1990, *Myxobolus* sp. II of Yemmen et al. (2012), and *Myxobolus* sp. of Kim et al. (2013b). The parasite in study, however, differs from most of these species in specific morphological aspects. For instance, the myxospores of *M. rohdei* are thinner with fewer polar tubule coils (three to four in comparison to the five coils reported here), those of *Myxobolus* sp. II of Yemmen et al. (2012) are larger and spherical in shape, while those of *Myxobolus* sp. of Kim et al. (2013b) have a wider morphometric range and overall smaller polar capsules (see Suppl. file S1). In turn, morphological differentiation from *M. spinacurvatura* is hard to be performed, given that the measurements of the myxospores in study are overall within the morphometric range reported for this species. Despite the morphological likeness, distance estimation showed low similarity to *M. spinacurvatura* (92.8%), while revealing 100% and 99.9% of similarity to the SSU rDNA sequences of a *Myxobolus* sp. deposited in GenBank under the accession numbers MF118767 and MH392320. Both these sequences were obtained from infections in the gills of *M. cephalus*: the first from specimens originating from wild catches in the Spanish Mediterranean coast (isolate Spain1-g) (Sharon et al. 2019), and the second from specimens originating from the Samsun coasts of the Black Sea in Turkey (unpublished data in GenBank). All other SSU rDNA sequences included in the analysis showed similarity values lower than 98.0%. Considering all the above, this parasite is suggested as a new species, herein named *Myxobolus mugiliensis* n. sp., with the River Minho as type locality (Table 3). Other geographic localities were included in the summary provided as supplementary material (see Suppl. file S1).

Myxobolus vesicularis n. sp.

Diagnosis: Polysporic plasmodia located in the gall bladder wall. Myxospores ellipsoidal in valvular and sutural view, displaying 10 to 12 markings near the suture line. Two pyriform equally sized polar capsules located side by side at the anterior pole (Figs. 6c, d, 7k and Table 3).

Type host: The flathead grey mullet *Mugil cephalus* Linnaeus, 1758 (Teleostei, Mugilidae).

Type locality: The River Minho (41° 56′ N, 08° 45′ W), near "Vila Nova de Cerveira", Portugal.

Other localities: The Spanish Mediterranean coast.

Prevalence of infection: Three infected in ten specimens examined (30.0%).

Material deposited: Series of phototypes of the hapantotype, deposited together with a representative DNA sample in the Natural History and Science Museum of the University of Porto, Portugal, reference CIIMAR 2019.37.

Etymology: The specific epithet "*vesicularis*" refers to the organ of infection in which the parasite was observed.

Molecular data: One SSU rDNA gene sequence with a total of 1943 bp, representative of three identical sequences that were separately assembled from the partial results obtained from plasmodia in the gall bladder wall tissue of three infected specimens.

Remarks: Morphometry was determined from mature myxospores observed in all three infected hosts. Individual measurements were identical between case isolates, so no significant morphometric variation was recorded. Comparison to all other *Myxobolus* spp. previously reported from mullet hosts revealed the parasite falling within the morphometric range of *M. spinacurvatura*, while further sharing some morphological similarity with *Myxobolus* sp. II of Yemmen et al. (2012). The myxospores of the latter, however, differ from those in study in their spherical shape, smaller width and thinner polar capsules (see Suppl. file S1; Yemmen et al. 2012). In turn, differentiation from *M. spinacurvatura* could only be achieved based on molecular data of the SSU rDNA gene. Distance estimation revealed the parasite in study displaying only 92.0% of similarity to *M. spinacurvatura*, while sharing 99.9% of similarity to a *Myxobolus* sp. (MF118772) that was recently reported from infections in the gills and tail of *M. cephalus* originating from wild catches in the Spanish Mediterranean coast (isolate Spain5-i) (Sharon et al. 2019). The occurrence of infection in three distinct organs corroborates the histological findings of Sharon et al. (2019) that showed the parasite having specificity towards the connective tissue. Considering all the above, this parasite is suggested as a new species, herein named *Myxobolus vesicularis* n. sp., with the connective tissue as site of infection and the River Minho as type locality (Table 3). Other geographic localities were included in the summary provided as supplementary material (see Suppl. file S1).

Myxobolus urinaris n. sp.

Diagnosis: Polysporic plasmodia located in the urinary bladder. Myxospores ellipsoidal in valvular view, with two pyriform equally sized polar capsules located side by side at the anterior pole (Figs. 6e, f, 7l and Table 3).

Type host: The flathead grey mullet *Mugil cephalus* Linnaeus, 1758 (Teleostei, Mugilidae).

Type locality: The River Minho (41° 56′ N, 08° 45′ W), near "Vila Nova de Cerveira", Portugal.

Prevalence of infection: Two infected in ten specimens examined (20.0%).

Material deposited: Series of phototypes of the hapantotype, deposited together with a representative DNA sample in the Natural History and Science Museum of the University of Porto, Portugal, reference CIIMAR 2019.38.

Etymology: The specific epithet "*urinaris*" refers to the organ of infection in which the parasite was observed.

Molecular data: One SSU rDNA gene sequence with a total of 1958 bp, representative of two identical sequences that were separately assembled from the partial results obtained from plasmodia in the urinary bladder samples of two infected specimens.

Remarks: Morphometry was determined from mature myxospores observed in both infected hosts. Individual measurements were identical between case isolates, so no significant morphometric variation was recorded. Comparison to all other *Myxobolus* spp. previously reported from mullet hosts revealed some morphometric similarity to *M. exiguus*, *M. rohdei* and *Myxobolus* sp. of Kim et al. (2013b). The myxospores of *M. rohdei* can be differentiated from those of the parasite in study based on their bigger size and fewer number of polar tubule coils (see Suppl. file S1). In turn, morphological differentiation from *M. exiguus* and *Myxobolus* sp. of Kim et al. (2013b) is solely based on the absence of sutural markings in the myxospores in study, given that these three species share highly similar morphometric ranges (see Suppl. file S1; Kim et al. 2013b; Rocha et al. 2019a). The newness of the parasite described here, however, is confirmed by distance estimation analysis, which revealed similarity values lower than 98.0% to all SSU rDNA sequences analysed, including those of *M. exiguus* (85.9%) and *Myxobolus* sp. of Kim et al. (2013b) (94.0%). Thus, this parasite is suggested as a new species, herein named *Myxobolus urinaris* n. sp.

Myxobolus galaicoportucalensis n. sp.

Diagnosis: Polysporic plasmodia located in the intestine. Myxospores ellipsoidal in valvular and sutural view, displaying 12 to 14 markings near the suture line. Two pyriform equally sized polar capsules located side by side at the anterior pole (Figs. 6g, h, 7m and Table 3).

Type host: The flathead grey mullet *Mugil cephalus* Linnaeus, 1758 (Teleostei, Mugilidae).

Type locality: The River Minho (41° 56′ N, 08° 45′ W), near "Vila Nova de Cerveira", Portugal.

Other localities: The Spanish Mediterranean coast.

Prevalence of infection: Two infected in 10 specimens examined (20.0%).

Material deposited: Series of phototypes of the hapantotype, deposited together with a representative DNA sample in the Natural History and Science Museum of the University of Porto, Portugal, reference CIIMAR 2019.39.

Etymology: The specific epithet "*galaicoportucalensis*" refers to the parasite's type locality – the River Minho – marking the boundary between Portugal and Galicia (Spain).

Molecular data: One SSU rDNA gene sequence with a total of 1975 bp, representative of two identical sequences that were separately assembled from the partial results obtained from plasmodia in the intestine of two infected specimens.

Remarks: Morphometry was determined from mature myxospores observed in both infected hosts. Individual measurements were identical between case isolates, so no significant morphometric variation was recorded. Comparison to all other *Myxobolus* spp. previously reported from mullet hosts revealed the parasite falling within the morphometric range of *M. spinacurvatura*, while further sharing some morphological similarity with *Myxobolus* sp. II of Yemmen et al. (2012). The myxospores of the latter differ from those in study in being generally shorter and having thinner polar capsules (see Suppl. file S1). Differentiation from *M. spinacurvatura* could not be performed based on the morphological traits of the myxospores; however, distance estimation showed the parasite in study sharing only 92.3% of similarity with this species. This analysis further revealed 100% and 99.9% of similarity to the sequences of a *Myxobolus* sp. (MF118763, MF118768 and MF118766) that was recently reported from infected specimens of *M. cephalus* caught from the Spanish Mediterranean coast: MF118763 from the scales (isolate Spain7-s); MF118768 from the muscle (isolate Spain1-m); and MF118766 from the tail (Spain1-t) (Sharon et al. 2019). Considering all the above, this parasite is suggested as a new species, herein named *Myxobolus galaicoportucalensis* n. sp., with the River Minho as type locality (Table 3). All reported sites of infection and geographic localities were included in the summary provided as supplementary material (see Suppl. file S1). Still regarding distance estimation, a 99.6% similarity was further calculated in relation to the SSU rDNA sequence of the Sphaeractinomyxon type 2 of Rangel et al., 2016. Despite this high percentage of similarity, nucleotide comparison among the sequences revealed the few differing nucleotides bearing significance for species differentiation, given that they are spread throughout the sequence, with their positioning being consistent between all identical partial sequences. All other SSU rDNA sequences included in the analysis displayed similarity values lower than 98.0% to the parasite in study.

Occurrence of known species in the thinlip grey mullet *Chelon ramada*

Myxobolus exiguus Thélohan, 1895

This species was recently re-described from macroscopic cysts developing in the visceral peritoneum of *C. ramada* captured from this same study area (see Rocha et al. 2019a). During this myxozoan survey, myxospores of *M. exiguus* could also be morphologically and molecularly identified in smears of the gall bladder (Fig. 8a, b) and intestine (Fig. 8c),

as a result of contamination due to the rupture of microscopic cysts in the visceral peritoneum.

Ellipsomyxa mugilis (Sitjà-Bobadilla and Álvarez-Pellitero, 1993)

Developmental stages of *E. mugilis* were found parasitizing the gall bladder of *C. ramada*, with a prevalence of infection of 22.7% (five infected in 22 specimens examined). Disporic plasmodia and mature myxospores were observed floating free in the bile (Fig. 8d–g). Young plasmodia appeared polymorphic, with an irregular cellular membrane due to the presence of pseudopodia throughout (Fig. 8d), while mature plasmodia appeared subspherical with smooth cellular membrane, each containing two immature myxospores (Fig. 8e). Mature myxospores were ellipsoidal, measuring 5.8 ± 0.2 (5.5–6.0) μm (n = 12) in length, 9.0 ± 0.7 (6.7–9.7) μm (n = 30) in width, and 12.0 ± 0.9 (11.1–14.0) μm (n = 30) in thickness. The suture line was laterally shifted and slightly curved, separating the two asymmetric valves. Two subspherical equally sized polar capsules, 4.0 ± 0.2 (3.5–4.0) μm long (n = 16) and 3.0 ± 0.3 (2.7–3.9) μm wide (n = 40), opened subterminally and in opposite directions, each containing a polar tubule coiled in six turns (Fig. 8f, g). One SSU rDNA gene sequence with a total of 1720 bp was deposited in GenBank with the accession no. MK193812. The latter is representative of five identical sequences that were separately assembled from the partial results obtained from plasmodia and myxospores in the gall bladder of five infected specimens. A voucher constituted by a series of phototypes and representative DNA sample of the hapantotype was deposited in the Natural History and Science Museum of the University of Porto, Portugal, reference CIIMAR 2019.40. The morphological features of the plasmodia and myxospores were overall congruent with those previously reported in the original species description by Sitjà-Bobadilla and Álvarez-Pellitero (1993), albeit our observations showing the polar tubule coiled in six turns instead of five. Molecular comparison further confirmed the identity of the parasite, which shared 99.8–100% of similarity with the three SSU rDNA sequences available for *E. mugilis* in GenBank. High similarity values were further obtained to the SSU rDNA sequences of *Ellipsomyxa syngnathi* Køie and Karlsbakk, 2009 (99.8%) and *Ellipsomyxa gobii* Køie, 2003 (99.6%), whereas all other *Ellipsomyxa* spp. displayed similarity values lower than 97.4%.

Phylogenetic analysis

ML, BI and MP analyses revealed the SSU rDNA sequences of the new species of *Myxobolus* clustering among all other congeners thus far molecularly reported from mullet hosts, forming a well-supported clade of mugiliform-infecting *Myxobolus* spp. (Fig. 9). The species described here from *C. ramada* and *C. labrosus* specifically clustered among all others that infect hosts of the genus *Chelon* (except for *M. ramadus* n. sp.), to form a well-supported subclade. All *Myxobolus* spp. that infect hosts of the genus *Mugil*, including those described here, also clustered together to form another well-supported subclade sister to the former. The SSU rDNA sequence of *M. ramadus* n. sp. appeared positioned alone at the basis of the two latter subclades. Nonetheless, the most basal position of the clade was occupied by *M. supamattayai*,

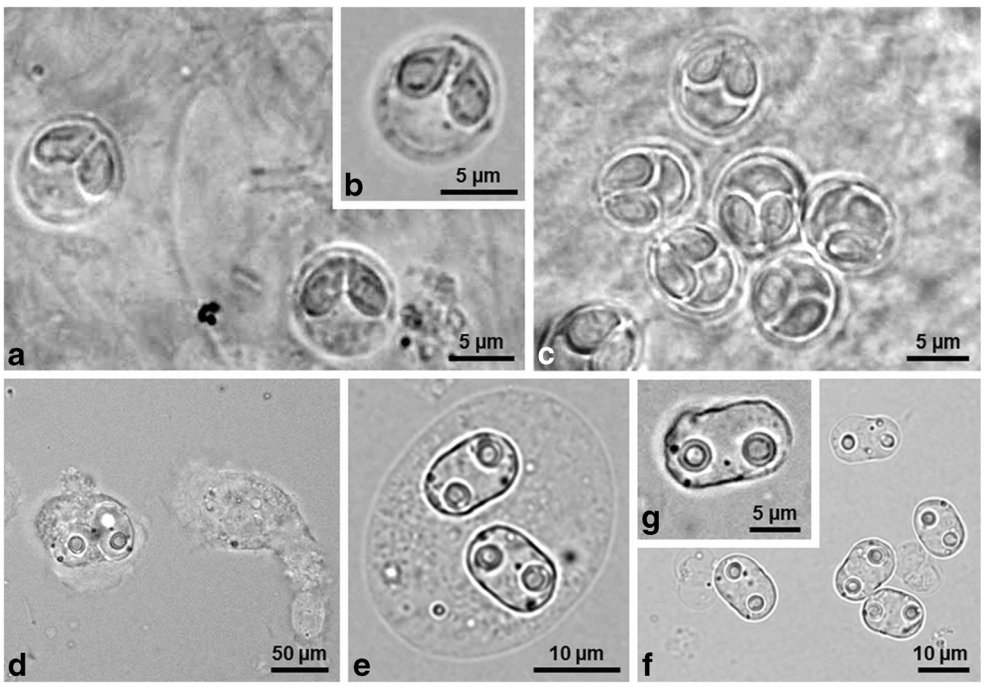

Fig. 8 Light micrographs of known myxosporean species infecting the thinlip grey mullet *Chelon ramada* in the River Minho. **a**–**c**. Myxospores of *Myxobolus exiguus* observed in smears of the gall bladder (**a**, **b**) and of the intestine (**c**), as a result of contamination due to the rupture of microscopic cysts in the visceral peritoneum. **d**–**g**. Disporic plasmodia and mature myxospores of *Ellipsomyxa mugilis*, coelozoic in the gall bladder: young plasmodia polymorphic, with cellular membrane irregular due to the presence of pseudopodia (**d**); mature plasmodia subspherical with smooth cellular membrane (**e**); mature myxospores floating free in the bile (**f**), and as observed in detail (**g**)

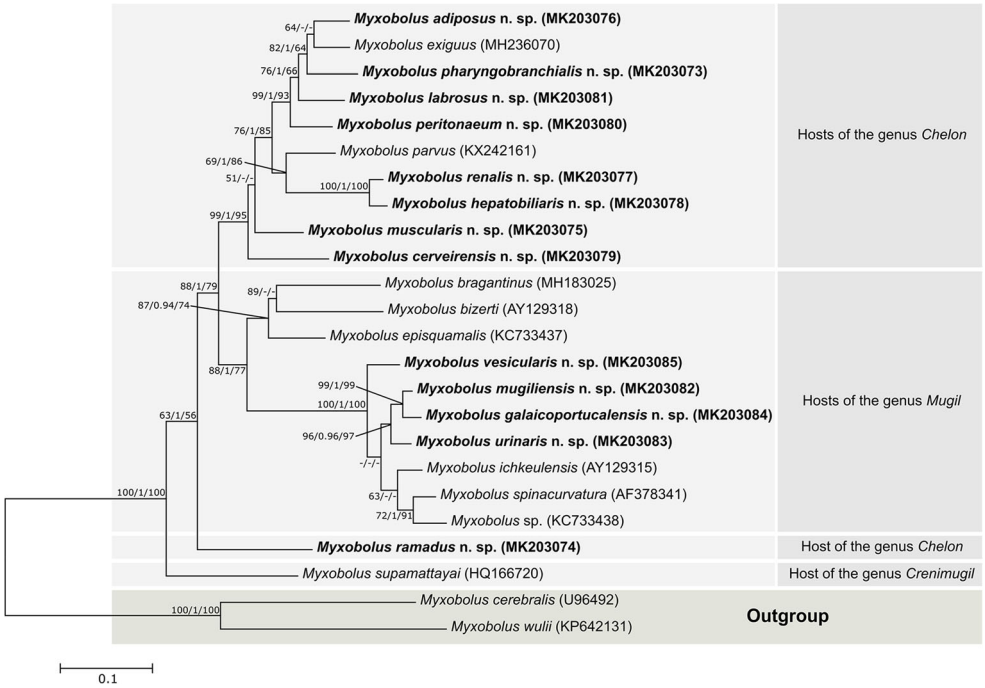

Fig. 9 Tree topology resulting from the maximum likelihood analysis of mugiliform-infecting *Myxobolus* spp., rooted to *Myxobolus cerebralis* (U96492) and *Myxobolus wulii* (KP642131). Number at the nodes are ML bootstrap values/BI posterior probabilities/MP bootstrap values; dashes represent a different branching pattern or a bootstrap support value under 50. The new *Myxobolus* spp. described in this study are marked using bold. Host groups are indicated using boxes.

this being the sole molecular representative of *Myxobolus* spp. that infect hosts of the genus *Crenimugil*.

Discussion

Myxozoan survey and description of new species

The reliable description of Myxosporea is currently accepted as being the result of the combined analysis of several criteria, namely myxospore morphology, host specificity, tissue of infection and molecular data (see Atkinson et al. 2015). Considering that phylogenetic studies widely show the vertebrate host group as the most relevant evolutionary signal for myxobolids (Ferguson et al. 2008; Carriero et al. 2013; Rocha et al. 2014), the species comparisons of *Myxobolus* performed in this study only took into consideration congeners reported from mugiliform fish hosts. Tissue tropism also constitutes an important evolutionary signal for myxobolids and other myxosporeans in general (see Eszterbauer 2004; Holzer et al. 2004; Ferguson et al. 2008). Nonetheless, the site of infection could not be used as an informative character for species comparison, considering that specific tissues of infection were not determined in this study, and neither is this type of information included in most descriptions of mugiliform-infecting *Myxobolus*. Future studies should, therefore, be careful to provide histological data for determining exact sites of infection. Overall, differentiation of the new *Myxobolus* spp. described here, among each other and in relation to congeners previously reported from mullets, was mainly based on molecular comparisons of SSU rDNA sequences. Morphology-based comparisons, however, remained necessary in order to establish differentiation from the many mugiliform-infecting *Myxobolus* spp. that are without available molecular data.

Although frequently necessary, the comparison of morphological traits for the identification of myxosporeans must be carried out cautiously. Phylogenetic studies have shown before that morphology-based criteria are unreliable for differentiation at the species-level. In the case of *Myxobolus*, the artificiality of the morphological criteria is evidenced by the numerous species of this genus that share similar myxospore shape and size, despite being molecularly different (see Atkinson et al. 2015). In this study, differentiation of *M. mugiliensis* n. sp., *M. vesicularis* n. sp. and *M. galaicoportucalensis* n. sp. from *M. spinacurvatura* could had not been performed without the help of molecular data, given that all these species have ellipsoidal myxospores with sutural markings, similar morphometric range and number of polar tubule coils. In the same manner, differentiation between *M. peritonaeum* n. sp. and *M. episquamalis* was only made possible by comparison of their respective SSU rDNA sequences. Thus, it can be stated that, without molecular input, these species could have been easily identified erroneously, consequently giving origin to species complexes. Molecular comparison of SSU rDNA sequences were further crucial in allowing differentiation between the several new species described here. For instance, *M. hepatobiliaris* n. sp. and *M. renalis* n. sp. from *C. ramada* share nearly identical myxospore morphology, however, differing in 2.7% of their SSU rDNA sequences. Similarly, the myxospores of *M. vesicularis* n. sp. and *M. galaicoportucalensis* n. sp. from *M. cephalus* are indistinguishable but differ in 5.7% of their

SSU rDNA sequences. High values of intraspecific variability have been reported for different isolates of a few *Myxobolus* spp. [e.g. *Myxobolus flavus* Carriero et al., 2013 (1.9%), and *Myxobolus koi* Kudo, 1919 (3.0%)] (Camus and Griffin 2010; Carriero et al. 2013). In the cases shown here, however, the possibility of high intraspecific variability was disregarded, considering that more than one SSU rDNA sequence was obtained for most of these species, being 100% identical among different isolates.

Overall, the new species described here showed high values of interspecific variability among each other, as well as to all other mugiliform-infecting congeners and actinosporean related sequences. Distance estimation revealed interspecific variability higher than 4% for the new *Myxobolus* spp. found infecting *C. ramada* and *M. cephalus*, and higher than 2% for those found in *C. labrosus*. Lower values of genetic difference (0.1%) and exact matches were obtained for *M. adiposus* n. sp., *M. mugiliensis* n. sp., *M. vesicularis* n. sp. and *M. galaicoportucalensis* n. sp. in relation to the SSU rDNA sequences of *Myxobolus* spp. that were mainly obtained from infected *M. cephalus* specimens captured from the Spanish Mediterranean coast (see Sharon et al. 2019). The lowest value of genetic difference calculated here and that possibly represents small interspecific variability was that of *M. galaicoportucalensis* n. sp. and the Sphaeractinomyxon type 2 of Rangel et al., 2016, which differed solely in 0.4% of their SSU rDNA sequences, corresponding to a total of eight different nucleotides. Nonetheless, sequence alignments showed that the position of the differing nucleotides bore significance for species differentiation, thus indicating it as possibly being representative of small interspecific variability. This is corroborated by the 100% of similarity that was calculated between the different geographic isolates of *M. galaicoportucalensis* n. sp. myxospores. On the other hand, it is also possible that this low genetic difference can be explained by ongoing processes of speciation in the vertebrate host due to host-shift and recombination of different lineages in annelid hosts (see Forró and Eszterbauer 2016), which would make it representative of intraspecific variability. Considering that life cycle inferences through molecular data should be performed cautiously, the genetic difference found between these two sequences is here prudently maintained as being representative of interspecific variability until further data arises. This result, however, reinforces the involvement of the sphaeractinomyxon collective group in the life cycles of mugiliform-infecting myxobolids, as hypothesized by Rocha et al. (2019b).

Most mugiliform-infecting *Myxobolus* spp. were originally described prior to the implementation and vulgarization of molecular procedures, consequently being without available molecular data. In fact, of the ca. 38 species of *Myxobolus* reported to infect mullets, only eight have molecular data available, plus a few SSU rDNA sequences belonging to unnamed *Myxobolus* spp. that infect *M. cephalus* (Kim et al. 2013b; Sharon et al. 2019). Of the above-mentioned eight species, only *Myxobolus bragantinus* Cardim et al. 2018 and *M. supamattayai* were originally described through combined morphological and molecular features (U-taynapun et al. 2011; Cardim et al. 2018). In turn, *Myxobolus bizerti* Bahri and Marques, 1996, *M. episquamalis*, *M. exiguus*, *M. ichkeulensis* and *M. spinacurvatura* were given molecular identity in subsequent reports from their original sites of infection and type hosts (Bahri et al. 2003; Rocha et al. 2019a). Only *M. parvus* was sequenced from a mullet species other than its type host. The molecular data available for this species was obtained from infections in the gills and kidney of leaping mullet *Chelon saliens* (Risso, 1810) from the Turkish coast of the Black Sea (Özer et al. 2016), despite it having been originally described from *M. cephalus* and so-iuy mullet *Planiliza haematocheila* (Temminck and Schlegel, 1845) off China (see Eiras et al. 2005). The occurrence of *M. parvus* in *C. saliens* therefore requires molecular validation through sequencing of the parasite from its type site of infection and host. Similarly, several other *Myxobolus* spp. have been reported from more than one mullet host on the basis of myxospore morphology (see Rocha et al. 2019a). Up until this study, however, none had been molecularly confirmed to infect more than a single mullet species. *Myxobolus adiposus* n. sp. now constitutes the sole exception, having molecular data available from infections that take place in *C. ramada* and *M. cephalus*. This confirms that host specificity of mugiliform-infecting *Myxobolus* is not restricted to a single host, with some species possibly having a cosmopolitan nature. In this context, providing molecular data for the many mugiliform-infecting *Myxobolus* spp. that have not been sequenced, specifically from their original site of infection and type host, constitutes an important task for future researches targeting myxozoans in mullets. The acquisition of this information is essential for both the reliable description of new *Myxobolus* spp. from these fishes, and for the recognition of the true host range of previously established species that have been reported from more than one mullet host.

Similarly, several mugiliform-infecting *Myxobolus* have been indiscriminately reported from a wide array of sites of infection (see Rocha et al. 2019a). Despite some species of this genus having been recognized to develop in different organs [e.g. *Myxobolus diaphanus* (Fantham et al., 1940), *Myxobolus cuneus* Adriano et al., 2006 and *Myxobolus cordeiroi* Adriano et al., 2009], this wide array of infection sites results from their specificity to the connective tissue (see Cone and Easy 2005; Adriano et al. 2006, 2009). In this study, *M. adiposus* n. sp. is described from the adipose tissue in the ocular cavity and urinary bladder, having further been molecularly reported by Sharon et al. (2019) from infections in the gills, intestine and tail. *Myxobolus muscularis* n. sp. is also described from the heart and skeletal muscle based on

sequencing of the SSU rDNA gene from its different sites of infection in *C. ramada*. While the myxospores of *M. adiposus* n. sp. were significantly easy to morphologically differentiate from all others observed in this study due to their spherical shape and symmetric polar capsules, those of *M. muscularis* n. sp. shared significant morphological similarity with the myxospores of *M. pharyngobranchialis* n. sp. and *M. episquamalis*, and could only be distinguished based on molecular data. Thus, the validity of the occurrence of a single species in different organs should be based on sequencing of the SSU rDNA gene or other adequate molecular markers, rather than on myxospore morphology.

Taking into consideration all the above, the necessity of using molecular tools for the myxozoan survey of mullets is undisputable and will most certainly increase the biodiversity of *Myxobolus* spp. known from these fish hosts. Molecular approaches should, however, be mindful of the possibility of co-infections, so as to not produce assembled chimeric sequences. In this study, the occurrence of co-infection was determined in several of the specimens of *C. ramada* examined. In fact, six other potentially different *Myxobolus* spp. were further observed in this host: *Myxobolus* sp. 1 forming filamentous microscopic cysts in the afferent artery of the gill filaments; *Myxobolus* sp. 2 and *Myxobolus* sp. 3 appearing disseminated in the spleen; *Myxobolus* sp. 4 disseminated or forming plasmodia in the kidney; and *Myxobolus* sp. 5 and *Myxobolus* sp. 6 forming plasmodia and appearing disseminated in the intestine, respectively. Molecular characterization of these *Myxobolus* was not possible due to the lack of parasites isolates (see Table 2).

The myxospores of the two unidentified morphotypes occurring in the intestine differ significantly from all others observed in this study, as well as from those of previously known species, therefore, potentially representing two new species. In turn, the myxospores of the *Myxobolus* sp. 1 in the gills and the *Myxobolus* sp. 2 infecting the spleen are morphometrically very similar among each other, as well as to those of *M. hepatobiliaris* n. sp. and *M. renalis* n. sp., which despite sharing the overall same myxospore morphometry were distinguished through means of molecular procedures. A similar situation was noticed between the myxospores of the *Myxobolus* sp. 3 in the spleen, the *Myxobolus* sp. 4 in the kidney, *M. muscularis* n. sp. and *M. pharyngobranchialis* n. sp., which are also morphometrically similar among each other, albeit the two latter having been demonstrated to be molecularly different. Considering these cases, it can be hypothesized that the acquisition of isolated biological material belonging to the unidentified morphotypes in the gills, spleen and kidney may come to reveal yet four other potential new species parasitizing *C. ramada*, regardless of their overall morphological similarity. It should be noted, however, that the measurements of *Myxobolus* sp. 3 and *Myxobolus* sp. 4 are also similar to those of *M. exiguus*, so that the possibility of co-infection in the spleen and kidney due to rupture of microscopic cysts in the visceral peritoneum cannot be disregarded.

During this myxozoan survey, myxospores of *M. exiguus* could be morphologically and molecularly identified in smears of the gall bladder and intestine, as a result of contamination. In turn, myxospores resembling *M. adeli*, *M. episquamalis*, *M. ichkeulensis*, *M. nile*, and *M. rohdei* were never observed, despite these species having been reported from mugilids in the Western Mediterranean off Spain, based on morphological criteria of the myxospores (see Yurakhno and Ovcharenko 2014).

Only two myxozoan species not belonging to the genus *Myxobolus* were observed in this study, both occurring in *C. ramada*: the coelozoic *Ellipsomyxa mugilis* forming disporic plasmodia attached to the gall bladder wall, or floating in the bile alongside free mature myxospores; and a species belonging to an unidentified genus, histozoic in the intestinal wall. *Ellipsomyxa mugilis* was originally described as *Zschokkella mugilis* from the gall bladder of the mugilids *C. ramada*, *C. saliens* and *M. cephalus* in the Western Mediterranean off Spain (Sitjà-Bobadilla and Álvarez-Pellitero 1993). Since then, this parasite was further reported from *C. saliens* off the Mediterranean coast of Tunisia (Thabet et al. 2016), as well as from actinosporean stages developing in the polychaete *Hediste diversicolor* in the Portuguese Atlantic coast, more specifically in the Aveiro estuary (Rangel et al. 2009), which is located about 175 km south from the estuary of the River Minho. In this study, the identification of *E. mugilis* was based on both myxospore morphology and molecular data of the SSU rDNA gene. Besides providing confirmation of species identity, molecular comparisons further revealed low genetic difference to the SSU rDNA sequences of *E. syngnathi* (0.2%) and *E. gobii* (0.4%). This low interspecific variability agrees with previously reported values (see Køie and Karlsbakk 2009; Thabet et al. 2016). Currently, these three species are distinguished based on morphological details of the myxospores, and narrow vertebrate host specificity. *Ellipsomyxa mugilis* and *E. gobii* further differ in actinospore morphometry (Køie 2000; Køie et al. 2004; Køie and Karlsbakk 2009; Rangel et al. 2009). A more comprehensive microscopic and molecular analysis of these three species is obviously necessary in order to either reinforce their differentiation or to reveal then as being cryptic. In turn, the data acquired for the non-myxobolid parasite infecting the intestine of *C. ramada* is, at this point, insufficient for genus determination and species characterization, so that further studies will be required.

The myxosporean species *Kudoa trifolia*, *K. unicapsula* and *Sphaerospora mugilis*, and a species of the genus *Alataspora* were also originally described from mullet hosts in the Western Mediterranean off Spain (Sitjà-Bobadilla and Álvarez-Pellitero 1993, 1995; Holzer et al. 2006; Yurakhno et al. 2007; Yurakhno and Ovcharenko 2014), with Yurakhno

and Ovcharenko (2014) further reporting the occurrence of *Enteromyxum leei*, *Sphaeromyxa sabrazesi*, *Kudoa dicentrarchi* and *Zschokkella admiranda* in mugilids of this geographic location, based on morphological criteria. Despite the geographic proximity, none of these species were found infecting the specimens of mullets examined here from the River Minho, which can possibly be related to differences in the composition of the invertebrate communities inhabiting the Western Mediterranean Sea and the Portuguese estuaries and coastal waters of the North Atlantic Ocean.

Species-richness of *Myxobolus* in mullets

About 38 species of *Myxobolus* have been reported to infect mullets worldwide (Marcotegui and Martorelli 2017; Cardim et al. 2018; Rocha et al. 2019a). This study adds 13 new species to this list from infections found in *C. ramada*, *C. labrosus* and *M. cephalus* captured from the River Minho, in Northern Portugal. The occurrence of unidentified myxospores in several organs of *C. ramada*, potentially belonging to new species, suggests that this already high biodiversity can, in fact, be increased by further pursuing myxozoan surveys in mullet hosts.

Prior to this study, only *M. exiguus* and *M. mugchelo* had been reported to occur in *C. ramada*, among other fish hosts. After being originally described by Thélohan (1895) from the stomach epithelium, pyloric caeca, kidney, and spleen of *C. ramada* and *C. labrosus*, as well as from the gills of the cyprinid *Abramis brama* (Linnaeus, 1758), *M. exiguus* was subsequently reported from a wide range of sites of infection and host species, clearly indicating it as a species complex. To resolve this issue, a recent study re-described *M. exiguus* from infections taking place in *C. ramada* captured from the River Minho, with this mullet species being settled as type species, and the visceral peritoneum as type tissue (Rocha et al. 2019a). The data presented here, which stems from the myxozoan survey from which the re-description of *M. exiguus* was performed, revealed the parasite occurring in all specimens of *C. ramada* examined posteriorly. This indicates that the prevalence of infection of this parasite in *C. ramada* is probably higher than that reported in its re-description, as microscopic cysts in the visceral peritoneum may pass unnoticed or be easily confused as a co-infection in organs of the visceral cavity.

In turn, *M. mugchelo* was originally described from the mesentery of *C. labrosus* from Italy, and recently reported from the intestinal wall of *C. ramada* from the same geographic location (Eiras et al. 2005; Ovcharenko et al. 2017). In this study, myxospores displaying the petite morphometric features reported for *M. mugchelo* were not observed in both *C. ramada* and *C. labrosus*, suggesting that this species may be absent in this specific geographic region. Nonetheless, it cannot be disregarded that only a few specimens of *C. labrosus* were examined in this study, so that further myxozoan surveys can come to disclose the presence of *M. mugchelo* in the River Minho. Still regarding *C. labrosus*, the description of *M. peritonaeum* n. sp. and *M. labrosus* n. sp. increases to five the number of *Myxobolus* spp. thus far reported from this mullet species, which is also the host for *M. parenzani* developing in the gills, as well as a possible host for *M. exiguus*, both reported on the basis of myxospore morphometry (see Rocha et al. 2019a). Consequently, the molecular data presented here for *M. peritonaeum* n. sp. and *M. labrosus* n. sp. constitutes the first available in GenBank for *Myxobolus* infections occurring in *C. labrosus*.

Mugil cephalus constitutes the mullet species from which a higher number of *Myxobolus* spp. have been reported, now accounting for ca. 23 species of this genus. It has been suggested that the *Myxobolus*-richness in *M. cephalus* probably reflects the higher number of myxozoan surveys that have been conducted on this mullet species, as a result of its economic importance for fisheries and aquaculture industries in several geographic locations (see Rocha et al. 2019a). Our study concurs with this assumption, given that myxozoan survey of *C. ramada* revealed a biodiversity of *Myxobolus* significantly higher than that expected upon consideration of the available literature. In comparison, *Myxobolus*-richness in *C. labrosus* was significantly low, but again, it cannot be disregarded that only a few specimens of this mullet species were examined, so that future myxozoan surveys targeting *C. labrosus* may increase its *Myxobolus* biodiversity.

In the past years, several studies have aimed to provide information regarding the biodiversity of myxozoans infecting mullets in specific geographic locations (e.g. Bahri and Marques 1996; Bahri et al. 2003; U-taynapun et al. 2011; Kim et al. 2013a, b; Yurakhno and Ovcharenko 2014; Özer et al. 2016; Thabet et al. 2016; Barreiro et al. 2017; Yang et al. 2017). Nonetheless, this study constitutes that from which a higher biodiversity of *Myxobolus* is reported. This probably relates to the careful morphological and molecular analyses that were performed here for species characterization, with no "pre-identification" at the species-level being performed based on myxospore morphology and morphometry. For instance, Özer et al. (2016) examined more than 200 specimens of leaping mullet *C. saliens* obtained from the Sinop coast of the Black Sea in a period of just over a year, but only identified infections by myxospores of *M. parvus* in several organs. Despite providing an SSU rDNA sequence from the parasite in the gills and kidney, reports of this species in the gall bladder and lower jaw of *C. saliens* were solely based on myxospore morphology, with the authors even acknowledging some morphological difference of the myxospores observed in the gall bladder. Similarly, Yurakhno and Ovcharenko (2014) examined ca. 450 specimens of *C. auratus* captured from the Mediterranean, Black

and Azov Seas during the course of two years, and described solely *M. adeli* from the intestine, pyloric caeca, eosophagus, stomach, swim bladder, gills and muscles, on the basis of myxospore morphometry. The broad array of organs displaying infection in both these cases, however, suggests that more than one *Myxobolus* spp. could have been present in the specimens analysed. Thus, the contrasting biodiversity of *Myxobolus* reported from mullets in different geographic localities may be essentially consequential to the use of poor discriminative criteria for identification at the species-level. U-taynapun et al. (2011) examined near 150 specimens of bluespot mullet *Moolgarda seheli* (Forsskål, 1775) captured from the Thailand coast of the Andaman Sea during the course of two years, and described only the blackish cysts of *M. supamatayai* developing in the skin, having found no microscopic signs of myxozoan infection in the other potential organs analysed. This shows that low biodiversity can also be related to the biological and ecological traits of the parasite and host vertebrate and invertebrate communities. Oligochaetes and polychaetes are the definitive and most ancient hosts of myxosporeans (Holzer et al. 2018); thus, it is reasonable to assume that the composition, spatial distribution, and susceptibility of the invertebrate community is determinant for the successful establishment and diversification of myxosporeans in different geographic locations.

Euryhaline hosts, such as anadromous and catadromous fishes, migrate between freshwater and marine habitats, passing through brackish waters during different periods of their lifetime. This capability of adaptation to different gradients of salinity allows migratory fish to interact with intrinsically different vertebrate and invertebrate communities, therefore making them potential temporary hosts for a wide array of myxozoan species that may develop in freshwater or marine annelids (e.g. Bartholomew et al. 1997, 2006; Rangel et al. 2017). Mullets are catadromous, meaning that they spawn in saltwater and then migrate into freshwater as juveniles, where they grow into adults before migrating back into the ocean. As such, mullets are potential temporary hosts for myxozoan species developing in oligochaetes or polychaetes, regardless being in freshwater, brackish or marine environments (Rocha et al. 2019b). Species of the genera *Myxobolus*, *Henneguya* Thélohan, 1892 and *Thelohanellus* Kudo, 1933 are the most commonly reported from freshwater habitats, less frequently occurring in brackish and marine habitats. These genera are known to display life cycles that involve freshwater oligochaetes, and possibly also marine oligochaetes, as invertebrate hosts (Eszterbauer et al. 2015; Rocha et al. 2019b). In this context, the lower biodiversity of *Myxobolus* reported in previous studies that targeted mullets in brackish/marine waters is probably consequential to the low availability of adequate invertebrate hosts for members of this myxosporean genus in those areas. In fact, this may also explain the significant variation of *Myxobolus*-richness that is reported here from *C. ramada*, *C. labrosus* and *M. cephalus*. In this study, the thinlip grey mullet *C. ramada* was undoubtedly the mullet species that displayed highest rate of *Myxobolus* infection, and by a significantly elevated number of different species. In accordance, it also constitutes that which more frequently is captured in upstream locations, as a result of its high adaptability to low salinities and water pollution (Cardona 2006); this being the reason why specimens of *C. ramada* were more frequently caught in our study area. Therefore, it can be hypothesized that the species that are able to tolerate lower salinity gradients are more prone to infection by myxobolids, as they interact more broadly with upstream benthic communities. Several studies have shown that species composition of annelid communities in Rivers and coastal waters is influenced by environmental factors, including salinity gradients (see Pfannkuche 1980; Pascar-Gluzman and Dimentman 1984; Moroz 1994; Seys et al. 1999; Schenková and Helešic 2006; Krodkiewska 2007; Armendáriz et al. 2011; Rosa et al. 2015; Kang et al. 2017). Future researches might aim to correlate the spatial distribution of mugiliform-infecting *Myxobolus* with that of its invertebrate hosts, and also to the migratory patterns of potential mullet hosts. Nonetheless, it will first be necessary to recognize full life cycles of these mugiliform-infecting *Myxobolus*, namely through the identification of invertebrate hosts; so that research in this field should aim to provide novel information on this subject.

Phylogenetic analysis

The phylogenetic analysis performed here is congruent with previously published phylograms of mugiliform-infecting *Myxobolus* spp. (e.g. Rocha et al. 2019a). Following the main phylogenetic trend of myxobolids to group in accordance with the vertebrate host taxonomic order (Ferguson et al. 2008; Carriero et al. 2013; Rocha et al. 2014), the SSU rDNA sequences of the new *Myxobolus* spp. described here cluster among congeners that have *bona fide* mugiliform fish hosts (see Rocha et al. 2019a), to form a well-supported clade of mugiliform-infecting *Myxobolus* spp. (Fig. 9). The inner topology of this clade further reveals tendency for species clustering in relation to host genus. Accordingly, the *Myxobolus* spp. that infect mullets of the genus *Chelon* form a well-supported subclade, sister to another well-supported subclade comprising species that infect mullets of the genus *Mugil*. Being the sole molecular representative of *Myxobolus* spp. that infect members of the genus *Crenimugil*, *M. supamattayai* stands alone, occupying the most basal position of the mugiliform-infecting *Myxobolus* clade. *Myxobolus ramadus* n. sp. constitutes the only exception to species clustering according to the host genus, appearing positioned alone at the basis of the two subclades separately comprising *Myxobolus* spp. that infect hosts of the genera *Chelon* and *Mugil*. This phylogenetic placement of

M. ramadus n. sp. shows that parasite host-switch has taken place between mugiliform genera. A contention that is further corroborated by the occurrence of *M. adiposus* n. sp. in *M. cephalus*, as reported by Sharon et al. (2019).

Phylogenetic studies have demonstrated that the origin and radiations of myxozoans reflect the evolution of their hosts (Carriero et al. 2013; Kodádková et al. 2015; Holzer et al. 2018; Patra et al. 2018). Despite the co-evolutionary history of this parasitic group and its vertebrate hosts being received as a "mixed signal" of invertebrate and vertebrate co-phylogeny due to the more ancient reciprocal adaptation of myxozoans and their definitive invertebrate hosts, the acquisition of vertebrates as alternate hosts was crucial for species diversification (Holzer et al. 2018). The phylogenetic analysis presented in this study agrees with this contention by revealing hyperdiversification of *Myxobolus* after entering mugiliform fish as alternate hosts. This high biodiversity probably reflects the processes of speciation that have led to the great ecological plasticity of mugiliform fish, which allows them to migrate and live, even if temporarily, in intrinsically distinct habitats, consequently entering in contact and feeding from a great variety of living organisms and materials. The placement of all new *Myxobolus* spp. described here within the previously known clade of mugiliform-infecting *Myxobolus* further supports the monophyletic origin of this group. Nonetheless, the results obtained in this study clearly show that the number of host-, site- and tissue-specific species in mullets is probably much higher than expected based on hitherto available literature, so that future myxozoan surveys may come to reveal other lineages of *Myxobolus* that evolved from distinct entries into mugiliform fish hosts.

Acknowledgements The authors acknowledge Professor Doutor Eduardo Rocha and the Laboratory of Histology of the Institute of Biomedical Sciences, University of Porto, for the usage of the Olympus BX50 light microscope, as well as Miguel Pereira for his assistance in figure preparation. This study was financially supported by FCT (Lisbon, Portugal) within the scope of the Ph.D. fellowship grant attributed to S. Rocha (SFRH/BD/92661/2013) through the programme QREN-POPH/FSE; and the Eng António de Almeida Foundation (Porto, Portugal). It complies with the current laws of the country in which it was performed.

Compliance with Ethical Standards

Conflict of interest On behalf of all authors, the corresponding author states that there is no conflict of interest.

References

Adriano EA, Arana S, Cordeiro NS (2006) *Myxobolus cuneus* n. sp. (Myxosporea) infecting the connective tissue of *Piaractus mesopotamicus* (Pisces: Characidae) in Brazil: histopathology and ultrastructure. Parasite 13:137–142. https://doi.org/10.1051/parasite/2006132137

Adriano EA, Arana S, Alves AL, Silva MR, Ceccarelli PS, Henrique-Silva S, Maia AA (2009) *Myxobolus cordeiroi* n. sp., a parasite of *Zungaro jahu* (Siluriformes: Pimelodiade) from Brazilian Pantanal: morphology, phylogeny and histopathology. Vet Parasitol 162:221–229. https://doi.org/10.1016/j.vetpar.2009.03.030

Almeida PR (2003) Feeding ecology of *Liza ramada* (Risso, 1810) (Pisces, Mugilidae) in a south-western estuary of Portugal. Estuar Coast Shelf Sci 57:313–323. https://doi.org/10.1016/S0272-7714(02)00357-8

Armendáriz LC, Capítulo AR, Ambrosio ES (2011) Relationships between the spatial distribution of oligochaetes (Annelida, Clitellata) and environmental variables in a temperate estuary system of South America (Río de la Plata, Argentina). N Z J Mar Fresh 45:263–279. https://doi.org/10.1080/00288330.2011.556652

Atkinson SD, Bartošová-Sojková P, Whipps CM, Bartholomew JL (2015) Approaches for characterising myxozoan species. In: Okamura B, Gruhl A, Bartholomew JL (eds) Myxozoan evolution, ecology and development. Springer International Publishing, Switzerland, pp 111–123

Bahri S, Marques A (1996) Myxosporean parasites of the genus *Myxobolus* from *Mugil cephalus* in Ichkeul lagoon, Tunisia: description of two new species. Dis Aquat Org 27:115–122. https://doi.org/10.3354/dao027115

Bahri S, Andree KB, Hedrick RP (2003) Morphological and phylogenetic studies marine *Myxobolus* spp. from mullet in Ichkeul Lake, Tunisia. J Eukaryot Microbiol 50:463–470. https://doi.org/10.1111/j.1550-7408.2003.tb00272.x

Barreiro L, Caamaño R, Cabaleiro S, Ruiz de Ocenda MV, Villoch F (2017) Ceratomyxosis infection in cultured striped red mullet (*Mullus surmuletus* Linnaeus, 1786) broodstock. Aquac Int 25:2027–2034. https://doi.org/10.1007/s10499-017-0166-6

Bartholomew JL, Whipple MJ, Stevens DG, Fryer JL (1997) The life cycle of *Ceratomyxa shasta*, a myxosporean parasite of salmonids, requires a freshwater polychaete as an alternate host. J Parasitol 83:859–868. https://doi.org/10.2307/3284281

Bartholomew JL, Atkinson SD, Hallett SL (2006) Involvement of *Manayunkia speciosa* (Annelida: Polychaeta: Sabellidae) in the life cycle of *Parvicapsula minibicornis*, a myxozoan parasite of Pacific salmon. J Parasitol 92:742–748. https://doi.org/10.1645/ge-781r.1

Camus AC, Griffin MJ (2010) Molecular characterization and histopathology of *Myxobolus koi* infecting the gills of a koi, *Cyprinus carpio*, with an amended morphological description of the agent. J Parasitol 96:116–124. https://doi.org/10.1645/ge-2113.1

Cardim J, Silva D, Hamoy I, Matos E, Abrunhosa F (2018) *Myxobolus bragantinus* n. sp. (Cnidaria: Myxosporea) from the gill filaments of the redeye mullet, *Mugil rubrioculus* (Mugiliformes: Mugilidae), on the eastern Amazon coast. Zootaxa 4482:177–187. https://doi.org/10.11646/zootaxa.4482.1.9

Cardona L (2001) Non-competitive coexistence between Mediterranean grey mullet: evidence from seasonal changes in food availability, niche breadth and trophic overlap. J Fish Biol 59:729–744. https://doi.org/10.1111/j.1095-8649.2001.tb02376.x

Cardona L (2006) Habitat selection by grey mullets (Osteichthyes: Mugilidae) in Mediterranean estuaries: the role of salinity. Sci Mar 70:443–455

Carriero MM, Adriano EA, Silva MR, Ceccarelli PS, Maia AA (2013) Molecular phylogeny of the *Myxobolus* and *Henneguya* genera with several new South American species. PLoS One 8:e73713. https://doi.org/10.1371/journal.pone.0073713

Cone DK, Easy RH (2005) Supplemental diagnosis and molecular taxonomy of *Myxobolus diaphanus* (Fantham, Porter et Richardson, 1940) (Myxozoa) parasitizing *Fundulus diaphanus* (Cyprinodontiformes) in Nova Scotia, Canada. Folia Parasitol 52:217–222. https://doi.org/10.14411/fp.2005.029

Crosetti D (2016) Current state of grey mullet fisheries and culture. In: Crosetti D, Blaber S (eds) Biology, ecology and culture of grey mullets (Mugilidae). CRC Press, Boca Raton, FL, pp 398–450

Crosetti D, Cataudella S (1995) Grey mullet culture. In: Nash CE (ed) World animal science 34B: production of aquatic animals. Elsevier, Burlington, MA, USA, pp 271–288

Das MK (1996) Myxozoan and urceolarid ciliate parasites of wild and cultured *Liza parsia* in deltaic West Bengal. J Inland Fish Soc India 28:46–56

Durand JD, Shen KN, Chen WJ, Jamandre BW, Blel H, Diop K, Nirchio M, Garcia de León FJ, Whitfield AK, Chang CW, Borsa P (2012) Systematics of the grey mullets (Teleostei: Mugiliformes: Mugilidae): molecular phylogenetic evidence challenges two centuries of morphology-based taxonomy. Mol Phylogenet Evol 64:73–92. https://doi.org/10.1016/j.ympev.2012.03.006

Egusa S, Maeno Y, Sorimachi M (1990) A new species of Myxozoa, *Myxobolus episquamalis* sp. n. infecting the scales of the mullet, *Mugil cephalus* L. Fish Pathol 25:87–91. https://doi.org/10.3147/jsfp.25.87

Eiras JC, Molnár K, Lu YS (2005) Synopsis of the species of *Myxobolus* Bütschli, 1882 (Myxozoa: Myxosporea: Myxobolidae). Syst Parasitol 61:1–46. https://doi.org/10.1007/s11230-004-6343-9

Eszterbauer E (2004) Genetic relationship among gill-infecting *Myxobolus* species (Myxosporea) of cyprinids: molecular evidence of importance of tissue-specificity. Dis Aquat Org 58:35–40. https://doi.org/10.3354/dao058035

Eszterbauer E, Atkinson S, Diamant A, Morris D, El-Matbouli M, Hartikainen H (2015) Myxozoan life cycles: practical approaches and insights. In: Okamura B, Gruhl A, Bartholomew JL (eds) Myxozoan evolution, ecology and development. Springer International Publishing, Switzerland, pp 175–198

Faye N, Kpatcha TK, Debakate C, Fall M, Toguebaye BS (1999) Gill infections due to myxosporean (Myxozoa) parasites in fishes from Senegal with description of *Myxobolus hani* sp. n. Bull Eur Assoc Fish Pathol 19:14–16

Ferguson JA, Atkinson SD, Whipps CM, Kent ML (2008) Molecular and morphological analysis of *Myxobolus* spp. of salmonid fishes with the description of a new *Myxobolus* species. J Parasitol 94:1322–1334. https://doi.org/10.1645/ge-1606.1

Fiala I (2006) The phylogeny of Myxosporea (Myxozoa) based on small subunit ribosomal RNA gene analysis. Int J Parasitol 36:1521–1534. https://doi.org/10.1016/j.ijpara.2006.06.016

Forró B, Eszterbauer E (2016) Correlation between host specificity and genetic diversity for the muscle-dwelling fish parasite *Myxobolus pseudodispar*: examples of myxozoan host-shift? Folia Parasitol 63:019. https://doi.org/10.14411/fp.2016.019

Hallett SL, Diamant A (2001) Ultrastructure and small-subunit ribosomal DNA sequence of *Henneguya lesteri* n. sp. (Myxosporea), a parasite of sand whiting *Sillago analis* (Sillaginidae) from the coast of Queensland, Australia. Dis Aquat Org 46:197–212. https://doi.org/10.3354/dao046197

Hillis DM, Dixon MT (1991) Ribosomal DNA: molecular evolution and phylogenetic inference. Q Rev Biol 66:411–453. https://doi.org/10.1086/417338

Holzer AS, Sommerville C, Wootten R (2004) Molecular relationships and phylogeny in a community of myxosporeans and actinosporeans based on their 18S rDNA sequences. Int J Parasitol 34:1099–1111. https://doi.org/10.1016/j.ijpara.2004.06.002

Holzer AS, Blasco-Costa I, Sarabeev VL, Ovcharenko MO, Balbuena JA (2006) *Kudoa trifolia* sp. n. - molecular phylogeny suggests a new spore morphology and unusual tissue location for a well-known genus. J Fish Dis 29:743–755. https://doi.org/10.1111/j.1365-2761.2006.00770.x

Holzer AS, Bartošová-Sojková P, Born-Torrijos A, Lövy A, Hartigan A, Fiala I (2018) The joint evolution of the Myxozoa and their alternate hosts: a cnidarian recipe for success and vast biodiversity. Mol Ecol 27:1651–1666. https://doi.org/10.1111/mec.14558

Hotos GN, Vlahos N (1998) Salinity tolerance of *Mugil cephalus* and *Chelon labrosus* (Pisces: Mugilidae) fry in experimental conditions. Aquaculture 167:329–338. https://doi.org/10.1016/S0044-8486(98)00314-7

Kang H, Bae M-J, Lee D-S, Hwang S-J, Moon J-S, Park Y-S (2017) Distribution patterns of the freshwater oligochaete *Limnodrilus hoffmeisteri* influenced by environmental factors in streams on a Korean nationwide scale. Water 9:921. https://doi.org/10.3390/w9120921

Karlsbakk E, Kristmundsson A, Albano M, Brown P, Freeman MA (2017) Redescription and phylogenetic position of *Myxobolus aeglefini* and *Myxobolus platessae* n. comb. (Myxosporea), parasites in the cartilage of some North Atlantic marine fishes, with notes on the phylogeny and classification of the Platysporina. Parasitol Int 66:952–959. https://doi.org/10.1016/j.parint.2016.10.014

Kim WS, Kim JH, Jang MS, Jung SJ, Oh MJ (2013a) Infection of wild mullet (*Mugil cephalus*) with *Myxobolus episquamalis* in Korea. Parasitol Res 112:447–451. https://doi.org/10.1007/s00436-012-3075-7

Kim WS, Kim JH, Oh MJ (2013b) Morphologic and genetic evidence for mixed infection with two *Myxobolus* species (Myxozoa: Myxobolidae) in grey mullets, *Mugil cephalus*, from Korean waters. Korean J Parasitol 51:369–373. https://doi.org/10.3347/kjp.2013.51.3.369

Kodádková A, Bartošová-Sojková P, Holzer AS, Fiala I (2015) *Bipteria vetusta* n. sp. - an old parasite in an old host: tracing the origin of myxosporean parasitism in vertebrates. Int J Parasitol 45:269–276. https://doi.org/10.1016/j.ijpara.2014.12.004

Køie M (2000) First record of an actinosporean (Myxozoa) in a marine polychaete annelid. J Parasitol 86:871–872. https://doi.org/10.1645/0022-3395(2000)086[0871:froaam]2.0.co;2

Køie M, Karlsbakk E (2009) *Ellipsomyxa syngnathi* sp. n. (Myxozoa, Myxosporea) in the pipefish *Syngnathus typhle* and *S. rostellatus* (Teleostei, Syngnathidae) from Denmark. Parasitol Res 105:1611–1616. https://doi.org/10.1007/s00436-009-1598-3

Køie M, Whipps CM, Kent ML (2004) *Ellipsomyxa gobii* (Myxozoa: Ceratomyxidae) in the common goby *Pomatoschistus microps* (Teleostei: Gobiidae) uses *Nereis* spp. (Annelida: Polychaeta) as invertebrate hosts. Folia Parasitol 51:14–18. https://doi.org/10.14411/fp.2004.002

Krodkiewska M (2007) The distribution of *Potamothrix bavaricus* (Oeschmann, 1913) (Oligochaeta) in anthropogenic freshwater habitats of an industrialised area (Upper Silesia, Poland). Limnologica 37:259–263. https://doi.org/10.1016/j.limno.2007.02.001

Kumar S, Stecher G, Tamura K (2016) MEGA7: molecular evolutionary genetics analysis version 7.0 for bigger datasets. Mol Biol Evol 33:1870–1874. https://doi.org/10.1093/molbev/msw054

Laffaille P, Feunteun E, Lefebvre C, Radureau A, Sagan G, Lefeuvre JC (2002) Can thin-lipped mullet directly exploit the primary and detritic production of European macrotidal salt marshes? Estuar Coast Shelf Sci 54:729–736. https://doi.org/10.1006/ecss.2001.0855

Lom J, Arthur JR (1989) A guideline for the preparation of species descriptions in Myxosporea. J Fish Dis 12:151–156. https://doi.org/10.1111/j.1365-2761.1989.tb00287.x

Marcotegui P, Martorelli S (2017) *Myxobolus saladensis* sp. nov., a new species of gill parasite of *Mugil liza* (Osteichthyes, Mugilidae) from Samborombón Bay, Buenos Aires, Argentina. Iheringia Ser Zool 107:e2017026. https://doi.org/10.1590/1678-4766e2017026

Moroz TG (1994) Aquatic oligochaeta of the Dnieper-Bug estuary system. Hydrobiologia 278:133–138. https://doi.org/10.1007/bf00142321

Mota M, Rochard E, Antunes C (2016) Status of the diadromous fish of the Iberian Peninsula: past, present and trends. Limnetica 35:1–18. https://doi.org/10.23818/limn.35.01

Nelson JS, Grande TC, Wilson MVH (2016) Fishes of the world, 5th edn. John Wiley & Sons, Hoboken, New Jersey, USA, p 752

Oren OH (1981) Aquaculture of Grey Mullets International Biological Programme. vol 26. Cambridge University Press, Cambridge, UK, p 507

Ovcharenko M, Dezfuli BS, Castaldelli G, Lanzoni M, Giari L (2017) Histological and ultrastructural study of *Myxobolus mugchelo* (Parenzan, 1966) with initial histopathology survey of the *Liza ramada* host intestine. Parasitol Res 116:1713–1721. https://doi.org/10.1007/s00436-017-5447-5

Özer A, Gürkanli CT, Özkan H, Acar G, Ciftci Y, Yurakhno V (2016) Molecular characterization and morphological aspects of *Myxobolus parvus* (Myxozoa) from *Liza saliens* (Mugilidae) off the Turkish Black Sea coasts. Parasitol Res 115:3513–3518. https://doi.org/10.1007/s00436-016-5115-1

Paperna I, Overstreet RM (1981) Parasites and diseases of mullets (Mugilidae). In: Oren OH (ed) Aquaculture of grey mullets. Cambridge University Press, Cambridge, pp 1–19

Pascar-Gluzman C, Dimentman C (1984) Distribution and habitat characteristics of Naididae and Tubificidae in the inland waters of Israel and the Sinai Peninsula. Hydrobiologia 115:197–205. https://doi.org/10.1007/BF00027917

Patra S, Bartošová-Sojková P, Pecková H, Fiala I, Eszterbauer E, Holzer AS (2018) Biodiversity and host-parasite cophylogeny of *Sphaerospora* (sensu stricto) (Cnidaria: Myxozoa). Parasit Vectors 11:347. https://doi.org/10.1186/s13071-018-2863-z

Pfannkuche O (1980) Distribution, abundance and life cycles of Oligochaeta from the marine hygropsammal with special reference to the Phallodrilinae (Tubificidae). Int Rev Hydrobiol 65:835–848. https://doi.org/10.1002/iroh.19800650607

Rangel LF, Santos MJ, Cech G, Székely C (2009) Morphology, molecular data, and development of *Zschokkella mugilis* (Myxosporea, Bivalvulida) in a polychaete alternate host, *Nereis diversicolor*. J Parasitol 95:561–569. https://doi.org/10.1645/GE-1777.1

Rangel LF, Rocha S, Casal G, Castro R, Severino R, Azevedo C, Cavaleiro F, Santos MJ (2017) Life cycle inference and phylogeny of *Ortholinea labracis* n. sp. (Myxosporea: Ortholineidae), a parasite of the European seabass *Dicentrarchus labrax* (Teleostei: Moronidae), in a Portuguese fish farm. J Fish Dis 40:243–262. https://doi.org/10.1111/jfd.12508

Rocha S, Casal G, Garcia P, Matos E, Al-Quraishy S, Azevedo C (2014) Ultrastructure and phylogeny of the parasite *Henneguya carolina* sp. nov. (Myxozoa), from the marine fish *Trachinotus carolinus* in Brazil. Dis Aquat Org 112:139–148. https://doi.org/10.3354/dao02794

Rocha S, Casal G, Rangel L, Castro R, Severino R, Azevedo C, Santos MJ (2015) Ultrastructure and phylogeny of *Ceratomyxa auratae* n. sp. (Myxosporea: Ceratomyxidae), a parasite infecting the gilthead seabream *Sparus aurata* (Teleostei: Sparidae). Parasitol Int 64:305–313. https://doi.org/10.1016/j.parint.2015.04.002

Rocha S, Azevedo C, Oliveira E, Alves Â, Antunes C, Rodrigues P, Casal G (2019a) Phylogeny and comprehensive revision of mugiliform-infecting myxobolids (Myxozoa, Myxobolidae), with the morphological and molecular redescription of the cryptic species *Myxobolus exiguus*. Parasitology 146:479–496. https://doi.org/10.1017/s0031182018001671

Rocha S, Rangel LF, Castro R, Severino R, Azevedo C, Santos MJ, Casal G (2019b) The potential role of the sphaeractinomyxon collective group (Cnidaria, Myxozoa) in the life cycle of mugiliform-infecting myxobolids, with the morphological and molecular description of three new types from the oligochaete *Tubificoides insularis*. J Invertebr Pathol 160:33–42. https://doi.org/10.1016/j.jip.2018.12.001

Ronquist F, Huelsenbeck JP (2003) MrBayes 3: Bayesian phylogenetic inference under mixed models. Bioinformatics 19:1572–1574. https://doi.org/10.1093/bioinformatics/btg180

Rosa BFJV, Martins RT, Alves RG (2015) Distribution of oligochaetes in a stream in the Atlantic Forest in southeastern Brazil. Braz J Biol 75:1–7. https://doi.org/10.1590/1519-6984.02313

Saleh MA (2006) Cultured aquatic species information programme (CASIP): *Mugil cephalus*. FAO, Rome, Italy

Sarkar NK (1989) *Myxobolus anili* sp. nov. (Myxozoa: Myxosporea) from a marine teleost fish *Rhinomugil corsula* Hamilton. Proc Zool Soc Calcutta 42:71–74

Sarkar NK (1999) Some new Myxosporidia (Myxozoa: Myxosporea) of the genera *Myxobolus* Butschli, 1882, *Unicapsula* Davis, 1942, *Kudoa* Meglitsch, 1947, *Ortholinea* Shulman, 1962 and *Neoparvicapsula* Gajevskaya, Kovaleva and Shulman, 1982. Proc Zool Soc Calcutta 52:38–48

Schenková J, Helešic J (2006) Habitat preferences of aquatic oligochaeta (Annelida) in the Rokytná River, Czech Republic – a small highland stream. Hydrobiologia 564:117–126. https://doi.org/10.1007/s10750-005-1713-0

Seys J, Vincx M, Meire P (1999) Spatial distribution of oligochaetes (Clitellata) in the tidal freshwater and brackish parts of the Schelde estuary (Belgium). Hydrobiologia 406:119–132. https://doi.org/10.1023/a:1003751512971

Sharon G, Ucko M, Tamir B, Diamant A (2019) Co-existence of *Myxobolus* spp. (Myxozoa) in gray mullet (*Mugil cephalus*) juveniles from the Mediterranean Sea. Parasitol Res 118:159–167. https://doi.org/10.1007/s00436-018-6151-9

Sitjà-Bobadilla A, Álvarez-Pellitero P (1993) *Zschokkella mugilis* n. sp. (Myxosporea, Bivalvulida) from mulltes (Teleostei, Mugilidae) of Mediterranean waters - light and electron-microscopic description. J Eukaryot Microbiol 40:755–764. https://doi.org/10.1111/j.1550-7408.1993.tb04471.x

Sitjà-Bobadilla A, Álvarez-Pellitero P (1995) Light and electron microscopic description of *Polysporoplasma* n. g. (Myxosporea: Bivalvulida), *Polysporoplasma sparis* n. sp. from *Sparus aurata* (L), and *Polysporoplasma mugilis* n. sp. from *Liza aurata* L. Eur J Protistol 31:77–89. https://doi.org/10.1016/s0932-4739(11)80360-3

Sousa R, Dias SC, Guilhermino L, Antunes C (2008) Minho River tidal freshwater wetlands: threats to faunal biodiversity. Aquat Biol 3:237–250. https://doi.org/10.3354/ab00077

Thabet A, Tlig-Zouari S, Al Omar SY, Mansour L (2016) Molecular and morphological characterisation of two species of the genus *Ellipsomyxa* Køie, 2003 (Ceratomyxidae) from the gall-bladder of *Liza saliens* (Risso) off Tunisian coasts of the Mediterranean. Syst Parasitol 93:601–611. https://doi.org/10.1007/s11230-016-9647-7

Thélohan P (1895) Recherches sur les myxosporidies. Bull Sci Fr Bel 4:100–394

Torricelli P, Tongiorgi P, Almansi P (1981) Migration of grey mullet fry into the Arno river: seasonal appearance, daily activity, and feeding rhythms. Fish Res 1:219–234. https://doi.org/10.1016/0165-7836(81)90026-6

U-taynapun K, Penprapai N, Bangrak P, Mekata T, Itami T, Tantikitti C (2011) *Myxobolus supamattayai* n. sp. (Myxosporea: Myxobolidae) from Thailand parasitizing the scale pellicle of wild mullet (*Valamugil seheli*). Parasitol Res 109:81–91. https://doi.org/10.1007/s00436-010-2223-1

Whipps CM, Adlard RD, Bryant MS, Lester RJ, Findlay V, Kent ML (2003) First report of three *Kudoa* species from eastern Australia: *Kudoa thyrsites* from mahi mahi (*Coryphaena hippurus*), *Kudoa amamiensis* and *Kudoa minithyrsites* n. sp. from sweeper (*Pempheris ypsilychnus*). J Eukaryot Microbiol 50:215–219. https://doi.org/10.1111/j.1550-7408.2003.tb00120.x

Yang C, Zhou Y, Zhao Y, Huang W, Huang C (2017) Erection of *Unicapsulocaudum mugilum* gen. et sp. nov. (Myxozoa: Ceratomyxidae) based on its morphological and molecular data. J Nat Hist 51:457–467. https://doi.org/10.1080/00222933.2017.1303096

Yemmen C, Ktari MH, Bahri S (2012) Parasitofauna of some mugilid and soleid fish species from Tunisian lagoons. Acta Adriat 52: 173–182

Yurakhno VM, Ovcharenko MO (2014) Study of Myxosporea (Myxozoa), infecting worldwide mullets with description of a new species. Parasitol Res 113:3661–3674. https://doi.org/10.1007/s00436-014-4031-5

Yurakhno VM, Ovcharenko MO, Holzer AS, Sarabeev VL, Balbuena JA (2007) *Kudoa unicapsula* n. sp (Myxosporea : Kudoidae) a parasite of the Mediterranean mullets *Liza ramada* and *L. aurata* (Teleostei : Mugilidae). Parasitol Res 101:1671–1680. https://doi.org/10.1007/s00436-007-0711-8

Zetina-Rejón MJ, Arreguín-Sánchez F, Chávez EA (2003) Trophic structure and flows of energy in the Huizache–Caimanero lagoon complex on the Pacific coast of Mexico. Estuar Coast Shelf Sci 57:803–815. https://doi.org/10.1016/S0272-7714(02)00410-9